DEVELOPMENT AND EVALUATION OF A MICROEMULSION-BASED TOPICAL GEL CONTAINING EBERCONAZOLE NITRATE AND MOMETASONE FUROATE FOR THE MANAGEMENT OF CUTANEOUS FUNGAL INFECTIONS

ANTHONY EBORO OBOT[1], DEEPTI AGGARWAL[2]
M.PHARMA STUDENT (DEPARTMENT OF PHARMACEUTICS), HR INSTITUTE OF PHARMACY, HRIT UNIVERSITY, GHAZIABAD, UTTAR PRADESH, INDIA[1],
ASSOCIATE PROFESSOR (FACULTY OF PHARMACEUTICAL SCIENCES) HR INSTITUTE OF PHARMACY, HRIT UNIVERSITY, GHAZIABAD, UTTAR PRADESH, INDIA[2]

ABSTRACT
Superficial fungal infections are widespread skin conditions that often cause itching, redness, scaling, and inflammation. Effective treatment requires a combination of antifungal and anti-inflammatory agents, yet many of these drugs suffer from poor water solubility, limiting their therapeutic potential. To overcome this challenge, the present study developed a microemulsion-based topical gel (microemulgel) incorporating eberconazole nitrate, a potent antifungal, and mometasone furoate, a corticosteroid with strong anti-inflammatory activity.

Solubility screening identified Capryol 90, Tween 80, and Transcutol P as suitable excipients. Pseudo-ternary phase diagrams were used to optimize a stable microemulsion, which was then incorporated into a Carbopol 940 gel base. The resulting formulation displayed clear appearance, skin-compatible pH, good spreadability, and strong physical stability. Compatibility studies confirmed that both drugs remained stable within the gel matrix. In vitro release experiments demonstrated sustained, diffusion-controlled drug release, ensuring prolonged therapeutic action. Antifungal evaluation against *Trichophyton rubrum* revealed that the microemulgel exhibited superior efficacy compared to plain drug suspensions and a marketed formulation.

Overall, the study successfully addressed the solubility limitations of eberconazole nitrate and mometasone furoate. The developed microemulgel proved to be a stable, effective, and patient-friendly topical delivery system, offering promising potential for the management of inflamed cutaneous fungal infections.

Keywords: Eberconazole Nitrate, Mometasone Furoate, Microemulgel, Capryol 90, Carbopol 940, *Trichophyton rubrum*, Topical Delivery.

INTRODUCTION
Superficial fungal infections are among the most frequent skin disorders, affecting keratinized tissues such as skin, hair, and nails. Dermatophytes like *Trichophyton*, *Microsporum*, and *Epidermophyton* are the main pathogens, though *Candida* and *Malassezia* species may also cause disease. Conditions such as tinea corporis, cruris, pedis, faciei, capitis, and onychomycosis typically present with itching, scaling, erythema, and discomfort, reducing quality of life [1]. In India, dermatophytosis has become increasingly chronic,

recurrent, and resistant to therapy. Warm, humid climate, overcrowding, reinfection, poor adherence, incomplete treatment, and misuse of steroid-containing topical combinations contribute to this trend. Corticosteroids suppress inflammation but fail to eradicate fungi, leading to atypical presentations and frequent relapse [2]. Hence, experts discourage their routine use in dermatophytosis. Topical antifungals remain the treatment of choice for localized infections, but efficacy depends on both the drug and its vehicle [3]. Many antifungal agents are lipophilic and poorly soluble in water, making conventional creams and ointments less effective due to inadequate solubilization, slow release, or poor patient acceptability. The stratum corneum acts as the main barrier to drug penetration, and formulation properties strongly influence release, hydration, spreadability, and compliance [4]. To address these limitations, this study developed a microemulsion-based gel containing eberconazole nitrate and mometasone furoate. Both drugs are highly lipophilic, making them suitable for microemulsion systems that enhance solubilization and topical delivery [5]. Drug release was assessed using a Franz diffusion cell with a dialysis membrane, representing in vitro release rather than direct dermal permeation [6]. Superficial fungal infections often trigger inflammation marked by erythema, itching, scaling, burning, and discomfort. Persistent scratching can damage the skin barrier, increase susceptibility to secondary infections, and reduce adherence to therapy [7]. While corticosteroids effectively control inflammation, their misuse in dermatophytosis may conceal symptoms without eliminating fungi, leading to recurrent or resistant disease [8]. Hence, antifungal–steroid combinations should only be prescribed under medical supervision. Eberconazole nitrate, an imidazole antifungal, inhibits lanosterol 14α-demethylase, disrupting ergosterol synthesis and fungal cell membranes [9 - 10]. It is active against dermatophytes, *Candida*, and *Malassezia* species, but its poor aqueous solubility and lipophilicity limit conventional topical formulations. Mometasone furoate, a potent corticosteroid, reduces inflammation via glucocorticoid receptor-mediated gene regulation. Despite low systemic absorption, prolonged or inappropriate use can cause local adverse effects such as skin thinning or pigmentation changes [11]. Like eberconazole, it is highly lipophilic, making lipid-based systems suitable for its delivery. In this study, eberconazole nitrate (1% w/w) and mometasone furoate (0.1% w/w) were incorporated into a formulation, though anti-inflammatory activity was not directly evaluated [12].

The rationale for combining these drugs lies in their complementary actions: antifungal activity from eberconazole and symptomatic relief from mometasone. Unlike earlier cream formulations, this work developed a microemulsion-based gel capable of stabilizing two poorly soluble drugs in a nanosized system . Microemulsions enhance solubilization and drug release but lack viscosity for topical use; incorporating them into a Carbopol 940 gel improves spreadability, retention, and stability [13]. A 3:1 surfactant/co-surfactant ratio was optimized through pseudo-ternary phase diagrams, ensuring formulation suitability. Accordingly, a microemulsion-based gel containing eberconazole nitrate and mometasone furoate was developed to improve the topical delivery of these poorly water-soluble drugs. A conceptual overview of superficial dermatophytosis, the intended pharmacological roles of both drugs, and the rationale for formulation development is presented in **Figure 1**.

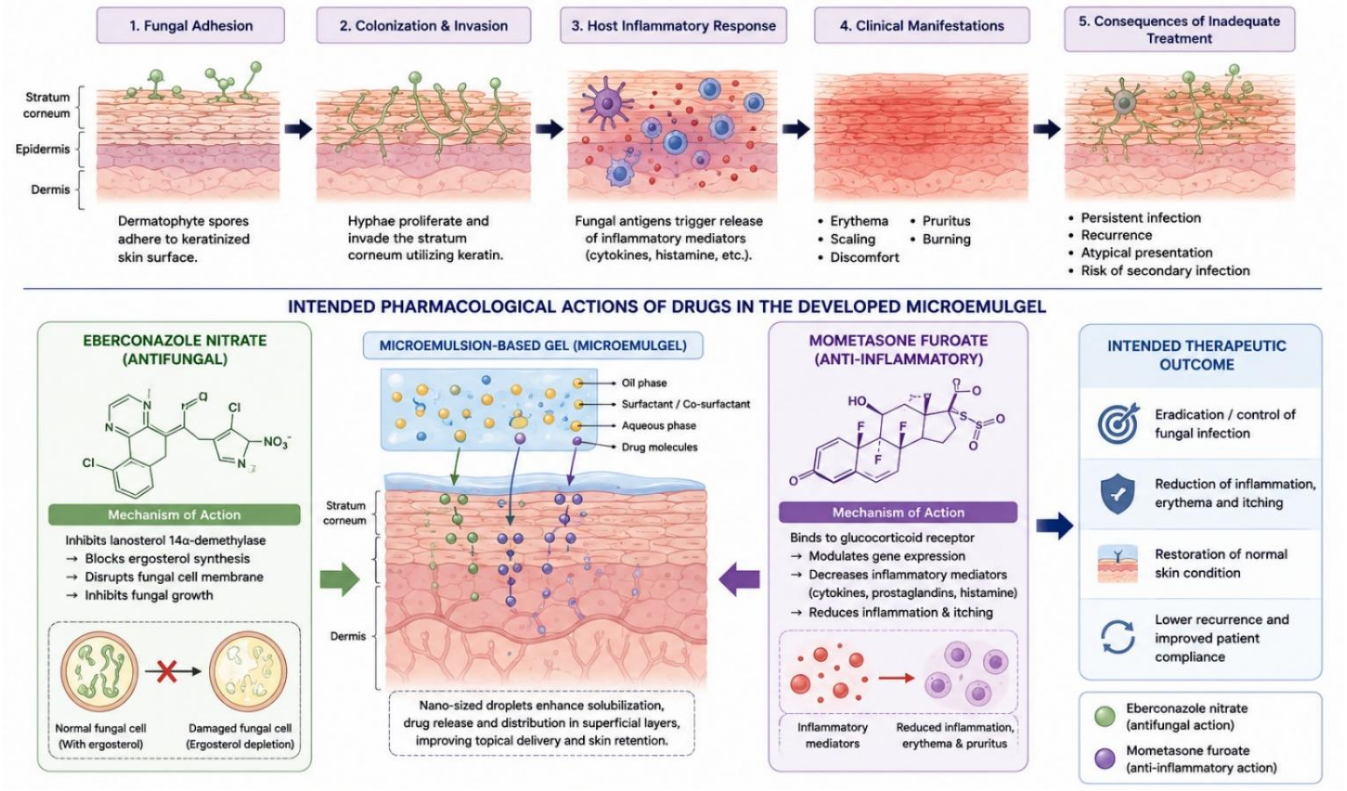

Figure.1: Conceptual illustration showing the progression of superficial dermatophytosis and the intended pharmacological actions of eberconazole nitrate (antifungal) and mometasone furoate (anti-inflammatory) in the developed microemulsion-based gel.

Formulation components were selected through solubility screening. Capryol® 90 served as the oil phase, while Tween® 80 and Transcutol® P were chosen as surfactant and co-surfactant due to their strong solubilizing ability for both eberconazole nitrate and mometasone furoate [14]. The surfactant/co-surfactant ratio was optimized using pseudo-ternary phase diagrams, and the resulting microemulsion was incorporated into a Carbopol® 940 gel to enhance viscosity, spreadability, and retention at the application site [15]. Although both drugs have been studied individually in topical preparations and conventional combination creams, little information exists on their simultaneous delivery through a microemulsion gel using the Capryol® 90–Tween® 80–Transcutol® P system. Moreover, data on the physicochemical properties, release behavior, and antifungal activity of such dual-drug microemulgels remain limited. This study therefore aimed to design and evaluate a microemulsion-based gel containing eberconazole nitrate and mometasone furoate, focusing on its physicochemical characteristics, in vitro drug release, and antifungal performance [16].

The work involved solubility studies, phase diagram construction, formulation optimization, and characterization of both the microemulsion and the final gel. Drug release was assessed using a Franz diffusion cell with a dialysis membrane, while antifungal activity was tested against *Trichophyton rubrum*. However, ex vivo permeation, dermal retention, anti-inflammatory activity, irritation studies, in vivo evaluation, and clinical testing were not included within the scope of this investigation.

1. MATERIALS AND METHOD

2.1 Materials

The active pharmaceutical ingredients and excipients used for the development of the microemulsion-based gel were selected based on their pharmaceutical suitability, reported safety for topical application, and compatibility with lipid-based delivery systems. Eberconazole nitrate and mometasone furoate were employed as the antifungal and anti-inflammatory agents, respectively. Capryol® 90 was used as the oil phase, Tween® 80 as the surfactant, Transcutol® P as the co-surfactant, and Carbopol® 940 as the gelling

agent [17]. Triethanolamine was used for neutralization of the gel base, while methanol, ethanol, and other solvents were used for analytical and formulation purposes. All chemicals and reagents were of analytical or HPLC grade and were used without further purification [18]. The active pharmaceutical ingredients, excipients, solvents, and microbiological media used in the present study are summarized in Table 1, Table 2 and Table 3.

Table.1: Active Pharmaceutical Ingredients Used in the Investigation

Material	Grade	Source	Purpose
Eberconazole nitrate	Pharmaceutical grade	Indiamart	Antifungal active pharmaceutical ingredient; used at 1.0% w/w
Mometasone furoate	Pharmaceutical grade	Indiamart	Intended anti-inflammatory active pharmaceutical ingredient; used at 0.1% w/w

Table. 2: Formulation Excipients and Screening Vehicles

Material	Grade	Source	Use in the investigation
Capryol® 90	Pharmaceutical grade	Merck, India	Selected oil phase
Isopropyl myristate	Pharmaceutical/Analytical grade	Merck, India	Oil screened during solubility studies
Oleic acid	Analytical grade	In-house	Oil screened during solubility studies
Labrafac Lipophile WL 1349	Pharmaceutical grade	Laboratory stock	Oil screened during solubility studies
Capmul® MCM	Pharmaceutical grade	Laboratory stock	Oil screened during solubility studies
Castor oil	Pharmaceutical grade	Local pharmacy	Oil screened during solubility studies
Tween® 80	Pharmaceutical/Analytical grade	Merck, India	Selected non-ionic surfactant
Tween® 20	Analytical grade	Merck, India	Surfactant screened during solubility studies
Cremophor® RH 40	Pharmaceutical grade	Laboratory stock	Surfactant screened during solubility studies
Kolliphor® EL	Pharmaceutical grade	Laboratory stock	Surfactant screened during solubility studies
Span® 80	Analytical grade	Laboratory stock	Surfactant screened during solubility studies
Transcutol® P	Pharmaceutical grade	Yarrow Chem Products, Mumbai, India*	Selected co-surfactant
Polyethylene glycol 400 (PEG 400)	Pharmaceutical/Analytical grade	Merck, India	Co-surfactant screened during solubility studies
Polyethylene glycol 200 (PEG 200)	Analytical grade	Merck, India	Co-surfactant screened during solubility studies
Propylene glycol	Pharmaceutical/Analytical grade	Merck, India	Co-solvent and humectant
Ethanol	Analytical grade	Merck, India	Co-solvent and analytical solvent
Carbopol® 940	Pharmaceutical grade	Loba Chemie Pvt. Ltd., India	Gelling polymer
Triethanolamine	Analytical grade	Merck, India	Neutralizing and pH-adjusting agent

Methyl paraben	Analytical grade	Loba Chemie Pvt. Ltd., India	Antimicrobial preservative
Propyl paraben	Analytical grade	Loba Chemie Pvt. Ltd., India	Antimicrobial preservative
Distilled water	Laboratory grade	Prepared in-house	Aqueous phase and formulation vehicle

Table. 3: Chemicals, Reagents, and Microbiological Materials

Material	Grade	Source	Purpose
Methanol	HPLC/Analytical grade	Merck, India	Preparation of stock solutions, extraction, dilution, and HPLC/UV analysis
Potassium dihydrogen phosphate	Analytical grade	Merck, India	Preparation of phosphate buffer
Sodium hydroxide	Analytical grade	Merck, India	pH adjustment of buffer and formulation
Hydrochloric acid	Analytical grade	Merck, India	pH adjustment where required
Phosphate-buffered saline (PBS, pH 7.4)	Laboratory prepared	Prepared in-house	Receptor medium for in vitro drug release studies
Potassium bromide (KBr)	Spectroscopic grade	Laboratory stock	Preparation of FTIR pellets
Sabouraud Dextrose Agar (SDA)	Microbiological grade	HiMedia Laboratories Pvt. Ltd., India	Revival and maintenance of *Trichophyton rubrum* culture
Sabouraud Dextrose Broth (SDB)	Microbiological grade	HiMedia Laboratories Pvt. Ltd., India	Broth microdilution medium for antifungal studies
Sterile Normal Saline	Sterile laboratory reagent	Prepared in-house	Preparation of fungal inoculum
Trichophyton rubrum	Authenticated laboratory culture	Departmental culture collection	Test organism for antifungal activity
Marketed topical formulation (Eberclin®, Batch No. EBE0017) *	Commercial product	Local pharmacy	Comparator in antifungal (MIC) study

1.2 Instruments and Equipment's

The instruments used for formulation development and characterization are presented in Table 4. All equipment was operated in accordance with standard laboratory procedures, and calibration or performance verification was carried out before use whenever required. Instrument model details were obtained from the corresponding equipment records and laboratory documentation. See the Table 4.

Table.4: Instruments and Equipment Used in the Investigation

Instrument/Equipment	**Manufacturer/Model**	**Main Use**
Analytical Balance	Shimadzu, Japan	Accurate weighing of drugs and excipients
Magnetic Stirrer with Hot Plate	REMI, India	Preparation of phase mixtures, microemulsions, and buffer solutions
Mechanical Stirrer	REMI, India	Preparation and homogenization of gel bases and microemulgels
Vortex Mixer	Laboratory model	Mixing of Smix and sample solutions
Orbital Shaker/Incubator	BR Biochem	Equilibrium solubility studies under controlled temperature and agitation
Centrifuge	REMI, India	Separation of undissolved drug and centrifugation studies
Ultrasonicator	PCI Analytics, India	Drug dissolution, sample extraction, and removal of entrapped air
UV–Visible Spectrophotometer	Shimadzu UV-1800	Wavelength scanning, calibration curve preparation, drug content, and in vitro release analysis

High-Performance Liquid Chromatography (HPLC)	Agilent 1260 Infinity II (PDA Detector)	Drug assay and analytical comparison
FTIR Spectrophotometer	Bruker	Drug identification and compatibility studies
Differential Scanning Calorimeter (DSC)	TA Instruments	Thermal characterization of drugs and formulations
X-ray Diffractometer (XRD)	Rigaku Corporation	Evaluation of crystalline and amorphous characteristics
Digital pH Meter	Eutech Instruments	Measurement of formulation pH
Refractometer	Laboratory model	Determination of refractive index of microemulsions
Brookfield Digital Viscometer	Brookfield Engineering, USA	Viscosity measurement of liquid and semisolid formulations
Particle Size and Zeta Potential Analyzer	Malvern Zetasizer Nano ZS	Determination of globule size, polydispersity index (PDI), and zeta potential
Vertical Franz Diffusion Cell Assembly	Electrolab, India	In vitro drug release studies using dialysis membrane
Hot Air Oven	Universal, India	Drying of glassware and temperature-controlled studies

2. EXPERIMENTAL DESIGN

The study followed a sequential formulation development approach involving drug characterization, solubility screening, pseudo-ternary phase diagram construction, formulation optimization, and evaluation. Based on solubility studies, Capryol® 90, Tween® 80, and Transcutol® P were selected as the oil, surfactant, and co-surfactant, respectively. A surfactant/co-surfactant (S_mix) ratio of 3:1, which provided the largest microemulsion region, was chosen for formulation development. Four microemulsion formulations (F1–F4) containing eberconazole nitrate (1% w/w) and mometasone furoate (0.1% w/w) were prepared and incorporated into a Carbopol® 940 gel base to obtain microemulgels. The formulations were evaluated for physicochemical properties, colloidal characteristics, in vitro drug release, and antifungal activity. The study was limited to laboratory-based formulation development and in vitro evaluation [11-12].

3.1 Preformulation Studies

Preformulation studies included evaluation of organoleptic properties, melting point, and UV absorption spectra of eberconazole nitrate and mometasone furoate. A simultaneous UV spectrophotometric method was developed and validated according to ICH guidelines for linearity, accuracy, precision, specificity, robustness, LOD, and LOQ. The validated method was used for drug content, in vitro release studies, and compared with HPLC assay results.

Equilibrium solubility studies were performed separately for eberconazole nitrate and mometasone furoate in various oils, surfactants, and co-surfactants using the shake-flask method. Based on the solubility data and formulation suitability, Capryol® 90 was selected as the oil phase, Tween® 80 as the surfactant, and Transcutol® P as the co-surfactant. The selected excipients exhibited superior solubilization capacity for both drugs and were therefore employed for subsequent pseudo-ternary phase diagram construction and microemulsion development [21].

Table 5. Vehicles screened during equilibrium solubility studies

Excipient class	Vehicles screened
Oils	Capryol® 90, Isopropyl myristate, Oleic acid, Labrafac Lipophile WL 1349, Capmul MCM, Castor oil
Surfactants	Tween® 80, Tween® 20, Cremophor RH 40, Kolliphor EL, Span® 80
Co-surfactants	Transcutol® P, PEG 400, PEG 200, Propylene glycol, Ethanol

3.2 Drug–Excipient Compatibility Studies

Drug–excipient compatibility was evaluated using Fourier transform infrared spectroscopy (FTIR), differential scanning calorimetry (DSC), and X-ray diffraction (XRD). FTIR spectra of the pure drugs, selected excipients, physical mixture, and optimized formulation were recorded using an ATR-FTIR spectrophotometer to identify any changes in characteristic functional groups [22]. Thermal behavior of the pure drugs and optimized formulation was assessed by DSC, whereas XRD analysis was performed to investigate changes in crystallinity after formulation. The obtained spectra and thermograms were compared to detect any evidence of physicochemical incompatibility or alteration in the solid-state properties of the drugs [23].

3.3 Construction of Pseudo-Ternary Phase Diagrams

Pseudo-ternary phase diagrams were constructed using the aqueous titration method to identify the microemulsion region. Tween® 80 and Transcutol® P were mixed at different weight ratios (1:1, 1:2, 2:1, 3:1, and 4:1) to prepare the surfactant/co-surfactant mixture (S_mix). Each S_mix ratio was combined with Capryol® 90 at different oil-to-S_mix ratios (1:9 to 9:1, w/w), followed by gradual addition of distilled water under continuous stirring. The compositions producing clear, transparent, and stable systems without phase separation were identified as the microemulsion region. The phase diagrams were generated using ternary diagram software, and the 3:1 Tween® 80: Transcutol® P ratio was selected for further formulation development owing to its largest microemulsion region [16-17].

Table.6: Variables used for pseudo-ternary phase diagram construction

Variable	Levels
Smix ratio	1:1, 1:2, 2:1, 3:1, 4:1 (Tween® 80: Transcutol® P)
Oil: Smix ratio	1:9–9:1 (w/w)
Aqueous phase	Distilled water
Selection criterion	Largest clear and stable microemulsion region

3.4 Preparation of Drug-Loaded Microemulsions

Four drug-loaded microemulsion formulations (F1–F4) were prepared by the spontaneous emulsification method using Capryol® 90 as the oil phase, Tween® 80 as the surfactant, and Transcutol® P as the co-surfactant. Eberconazole nitrate (1% w/w) and mometasone furoate (0.1% w/w) were dissolved in the oil phase, followed by the gradual addition of the surfactant/co-surfactant mixture under continuous magnetic stirring. Distilled water was then added dropwise until a clear and homogeneous microemulsion was obtained. The formulations were stirred for 30 min, sonicated for 10 min to remove entrapped air, and allowed to equilibrate at room temperature for 24 h before further evaluation [26].

Table 7. Composition of drug-loaded microemulsion formulations

Ingredient (% w/w)	F1	F2	F3	F4
Eberconazole nitrate	1.0	1.0	1.0	1.0
Mometasone furoate	0.1	0.1	0.1	0.1
Capryol® 90	8	10	12	14
Tween® 80	28	30	32	34
Transcutol® P	9	10	11	12
Distilled water	q.s.	q.s.	q.s.	q.s.

3.5 Evaluation of Drug-Loaded Microemulsions

The prepared microemulsions were evaluated for physicochemical properties, including clarity, transmittance, pH, conductivity, refractive index, viscosity, drug content, and physical stability, with results expressed as mean ± SD (n = 3). Drug content was determined by UV spectrophotometry after methanolic extraction. Stability was assessed by centrifugation, heating–cooling, and freeze–thaw cycles. Formulations showing no phase separation, precipitation, or visual changes were considered stable [27].

Table.8: Evaluation parameters for drug-loaded microemulsions

Parameter	Method
Visual appearance	Clarity, homogeneity, and phase separation
Percentage transmittance	UV–Visible spectrophotometer (650 nm)
pH	Digital pH meter
Electrical conductivity	Conductivity meter
Refractive index	Digital refractometer
Viscosity	Brookfield viscometer
Drug content	UV spectrophotometric analysis
Physical stability	Centrifugation, heating–cooling, and freeze–thaw studies

3.6 Preparation of Microemulgels

The optimized drug-loaded microemulsions (F1–F4) were converted into microemulgels using Carbopol® 940 as the gelling agent. Carbopol® 940 (1% w/w) was dispersed in purified water and allowed to hydrate for 24 h. Separately, methyl paraben (0.18% w/w) and propyl paraben (0.02% w/w) were dissolved in propylene glycol (10% w/w) and added to the hydrated gel under continuous stirring. The corresponding microemulsion was incorporated gradually into the Carbopol gel with gentle mechanical stirring until a homogeneous system was obtained. The pH was adjusted to 6.0–6.8 using triethanolamine to obtain the desired gel consistency. The prepared microemulgels were allowed to stand for 24 h to remove entrapped air and then stored in airtight containers until further evaluation [20 - 21].

Table.9: Composition of microemulgel formulations

Ingredient	Concentration (% w/w)	Function
Eberconazole nitrate	1.0	Antifungal drug
Mometasone furoate	0.1	Anti-inflammatory drug
Corresponding microemulsion (F1–F4)	q.s.	Drug delivery system
Carbopol® 940	1.0	Gelling agent
Propylene glycol	10.0	Humectant/Co-solvent
Methyl paraben	0.18	Preservative
Propyl paraben	0.02	Preservative
Triethanolamine	q.s.	Neutralizer/pH adjuster
Purified water	q.s.	Vehicle

3.7 Evaluation of Microemulgels

The prepared microemulgels were evaluated for their physicochemical properties, including appearance, homogeneity, grittiness, pH, viscosity, spreadability, extrudability, and drug content using standard analytical methods [30]. All measurements were performed in triplicate and expressed as mean ± SD. The pH was determined using a calibrated digital pH meter, viscosity was measured using a Brookfield viscometer, spreadability was evaluated by the parallel-slide method, and extrudability was determined by measuring the ease of gel extrusion from collapsible tubes under a fixed applied force. Drug content was determined by extracting the formulation with methanol followed by sonication, filtration, and UV spectrophotometric analysis using the validated simultaneous equation method. Selected formulation samples were also analyzed by HPLC for comparative assay determination [31].

3. SELECTION OF THE OPTIMIZED FORMULATION

The prepared formulations (F1–F4) were compared based on physicochemical characteristics, including clarity, pH, viscosity, drug content, spreadability, extrudability, and physical stability. The formulation exhibiting the most satisfactory overall performance was selected for further characterization. Based on the experimental findings, F3 was identified as the optimized formulation and was subjected to advanced physicochemical and in vitro evaluation.

4.1 Characterization of the Optimized Microemulsion

The optimized liquid microemulsion (F3) was characterized for mean globule size, polydispersity index (PDI), zeta potential, and morphology. Particle size, PDI, and zeta potential were determined using a Malvern Zetasizer Nano ZS after suitable dilution with distilled water. The morphology of the dispersed droplets was examined by transmission electron microscopy (TEM).

4.2 In Vitro Drug Release Study

The in vitro drug release of the optimized microemulgel was evaluated using a vertical Franz diffusion cell fitted with a dialysis membrane (MWCO 12,000–14,000 Da). Phosphate-buffered saline (PBS, pH 7.4) maintained at 37 ± 0.5°C served as the receptor medium under continuous stirring. Approximately 1 g of formulation was placed in the donor compartment. Samples were withdrawn at predetermined intervals up to 12 h, with an equal volume of fresh medium replaced after each withdrawal. Drug release was quantified using the validated UV spectrophotometric method.

4.3 Drug Release Kinetic Analysis

The release data obtained from the optimized formulation were fitted to Zero-order, First-order, Higuchi, Korsmeyer–Peppas, and Hixson–Crowell kinetic models. The model showing the highest coefficient of determination (R^2) was considered the best fit for describing the drug release behavior.

4.4 In Vitro Antifungal Activity

The antifungal activity of the optimized formulation was evaluated against *Trichophyton rubrum* using an adapted broth microdilution method. The formulation was compared with pure eberconazole nitrate and a marketed formulation. The minimum inhibitory concentration (MIC) was recorded as the lowest concentration showing complete inhibition of visible fungal growth after incubation.

4.5 Statistical Analysis

All experiments were carried out in triplicate, and the results were expressed as mean ± standard deviation (SD). Statistical analysis was performed using GraphPad Prism. Differences among formulations were analyzed using one-way ANOVA followed by Tukey's multiple comparison test, with $p < 0.05$ considered statistically significant.

4. RESULT AND DISCUSSION

The prepared microemulgel formulations (F1–F4) were evaluated for physicochemical properties, drug release, and antifungal activity. The obtained results are presented and discussed in the following sections. Among the tested formulations, F3 demonstrated the most satisfactory overall performance and was selected for further characterization.

5.1 Preformulation Results

5.1.1 Organoleptic Characteristics

The two active ingredients were examined before formulation. Both samples showed the expected white or off-white crystalline appearance and were free from visible contamination, discolouration, or abnormal odour. The final excipients used in the formulation also showed their expected physical appearance and were considered suitable for experimental use.

Table.10: Organoleptic Characteristics of the Active Ingredients and Final Formulation Excipients

Material	Appearance	Colour	Odour	Physical State	Observation
Eberconazole nitrate	Fine crystalline powder	White to off-white	Odourless	Solid	Complied
Mometasone furoate	Fine crystalline powder	White	Odourless	Solid	Complied
Capryol® 90	Clear oily liquid	Colourless to pale yellow	Mild characteristic	Liquid	Complied
Tween® 80	Viscous liquid	Pale yellow	Characteristic	Liquid	Complied
Transcutol® P	Clear liquid	Colourless	Mild characteristic	Liquid	Complied
Carbopol® 940	Fine fluffy powder	White	Odourless	Solid	Complied
Triethanolamine	Clear viscous liquid	Colourless	Mild characteristic	Liquid	Complied
Propylene glycol	Clear viscous liquid	Colourless	Odourless	Liquid	Complied
Methyl paraben	Crystalline powder	White	Odourless	Solid	Complied
Propyl paraben	Crystalline powder	White	Odourless	Solid	Complied

Figure.2: Organoleptic appearance of eberconazole nitrate and mometasone furoate recovered from the experimental record.

The appearance of the two drugs was consistent with the descriptions used for their preliminary identification. Organoleptic examination alone cannot establish chemical identity or purity, but it provides a useful first check before instrumental analysis.

4.2 Melting-Point Results

The observed melting points fell within the recorded reference ranges. Eberconazole nitrate melted at 166.3 ± 0.5°C, while mometasone furoate melted at 222.1 ± 0.7°C. The close agreement supported the preliminary identity and acceptable purity of the materials. These results were also consistent with the thermal events later observed by DSC.

Table.11: Melting Points of the Pure Drugs

Drug	Reported range (°C)	Observed value (°C)
Eberconazole nitrate	164–168	166.3 ± 0.5
Mometasone furoate	220–224	222.1 ± 0.7

5.3 UV-Visible Method Development and Validation Results

5.3.1 Absorption maxima and spectral overlap

EBZ showed its maximum absorbance at 261 nm, while MF showed its maximum at 248 nm. The spectra overlapped markedly between approximately 230 and 280 nm. This overlap confirmed that a single-wavelength measurement could not reliably assign the mixed response to one drug, supporting the use of the simultaneous-equation method.

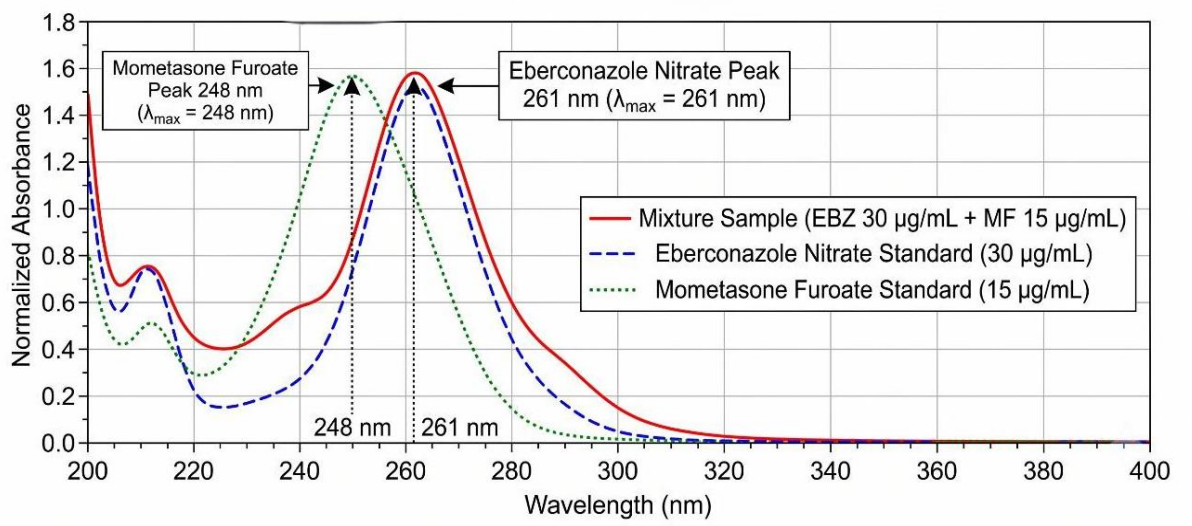

Figure. 3: Normalized overlain UV spectra of eberconazole nitrate, mometasone furoate, and their mixture in methanol. The curves illustrate spectral overlap and the selected wavelengths but were not used for quantitative calculations.

The normalized plot was prepared for visual comparison. Quantitative work used the absolute absorbances recorded at 261 and 248 nm. The calibration response at the primary wavelengths was approximately 0.648 for 30 µg/mL EBZ at 261 nm and 0.518 for 15 µg/mL MF at 248 nm.

5.4 Linearity and cross-absorptivity

EBZ showed linear absorbance over 10-50 µg/mL, while MF showed linear absorbance over 1-25 µg/mL. Each drug was measured at both wavelengths to obtain the four calibration-slope coefficients required for mixture resolution.

Table.12: Cross-Absorptivity Calibration Dataset (Mean ± SD, n = 3)

Drug	Concentration (µg/mL)	Absorbance at 261 nm (Mean ± SD)	Absorbance at 248 nm (Mean ± SD)
Eberconazole nitrate	10	0.218 ± 0.002	0.126 ± 0.001
	20	0.433 ± 0.003	0.251 ± 0.002
	30	0.648 ± 0.004	0.376 ± 0.003
	40	0.863 ± 0.005	0.501 ± 0.004
	50	1.078 ± 0.006	0.626 ± 0.005
Mometasone furoate	1	0.020 ± 0.001	0.039 ± 0.001
	5	0.092 ± 0.001	0.176 ± 0.002
	10	0.182 ± 0.002	0.347 ± 0.003
	15	0.272 ± 0.002	0.518 ± 0.004
	20	0.362 ± 0.003	0.689 ± 0.005
	25	0.452 ± 0.004	0.860 ± 0.006

Table.13: Four-Wavelength Regression Statistics and Absorptivity Coefficients

Parameter	EBZ at 261 nm	EBZ at 248 nm	MF at 261 nm	MF at 248 nm
Range (µg/mL)	10-50	10-50	1-25	1-25
Regression equation	y = 0.0215x + 0.003	y = 0.0125x + 0.001	y = 0.0180x + 0.002	y = 0.0342x + 0.005
Slope coefficient	0.0215	0.0125	0.0180	0.0342
Intercept	0.003	0.001	0.002	0.005
R^2	0.9991	0.9989	0.9992	0.9995

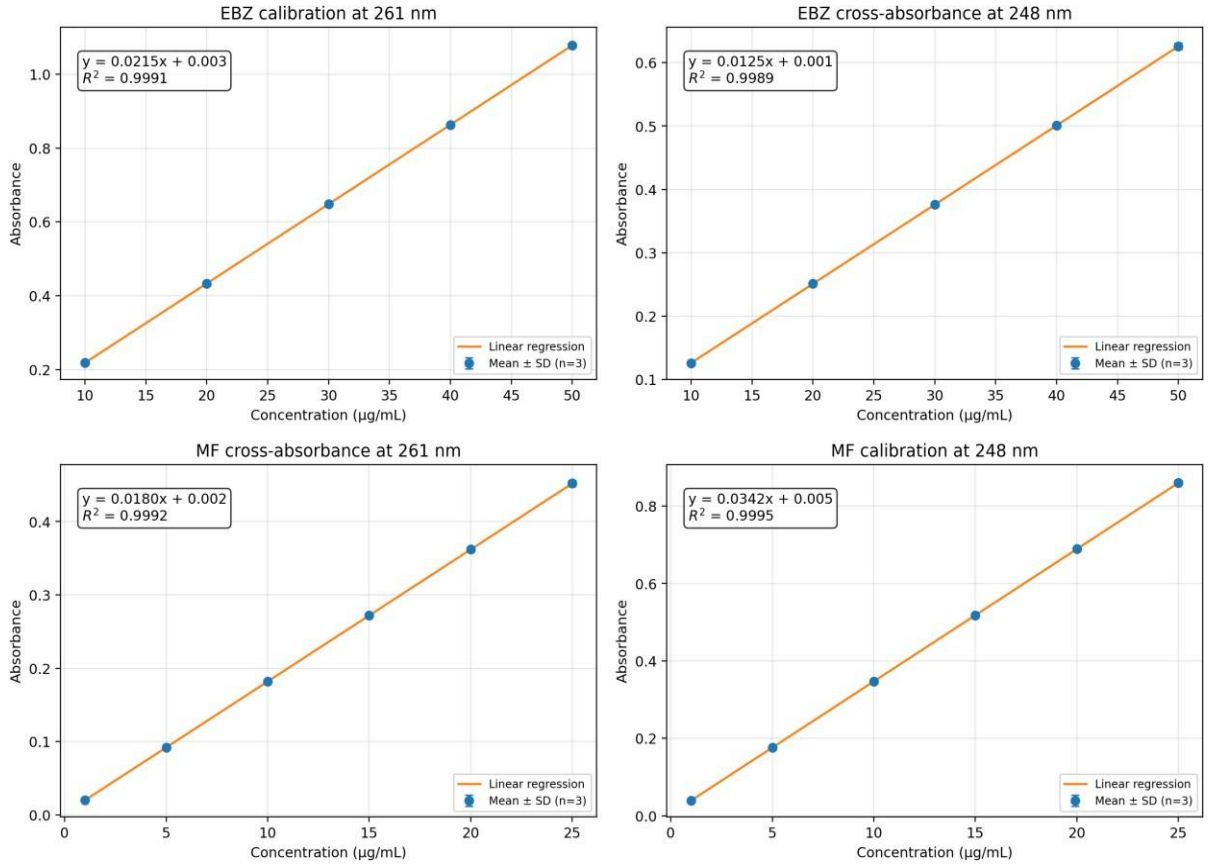

Figure.4: Calibration and cross-absorbance curves for EBZ and MF at 261 and 248 nm (mean± SD, n = 3).

All four regressions showed strong linearity. The coefficients used in the simultaneous equations were a_{x1} = 0.0215, a_{x2} = 0.0125, $a_{\gamma1}$ = 0.0180, and $a_{\gamma2}$ = 0.0342. The lower MF calibration limit of 1 µg/mL addressed the ten-fold lower MF concentration in the formulation.

5.5 Selectivity and laboratory-mixture recovery

The methanol blank gave zero absorbance at both wavelengths. The pH 7.4 receptor medium gave absorbances of 0.0021 at 261 nm and 0.0030 at 248 nm, while the placebo extract gave 0.0042 and 0.0045, respectively. These low matrix responses were accounted for by blank correction before mixture calculations.

Table.14: Recovery from Laboratory-Prepared EBZ-MF Mixtures (n = 3)

Mixture	Actual EBZ:MF (µg/mL)	Calculated EBZ:MF (µg/mL)	EBZ recovery (%)	MF recovery (%)
10:1 target	20.0:2.0	20.12:1.97	100.6 ± 0.82	98.5 ± 1.14
Higher MF	20.0:3.0	19.85:3.04	99.2 ± 0.95	101.3 ± 1.05
Low-level 10:1	10.0:1.0	9.92:1.02	99.2 ± 1.10	102.0 ± 1.35

The recoveries remained close to 100% across the tested ratios, indicating that the two equations could resolve EBZ and MF in laboratory-prepared mixtures, including the target 10:1 ratio.

5.6 Accuracy, precision, and sensitivity

Table.15: Accuracy of the Simultaneous-Equation Method

Drug	Spike level	Amount added (µg/mL)	Mean recovery (%)	SD	%RSD
EBZ	80%	16.0	99.73	0.91	0.91
EBZ	100%	20.0	100.35	0.96	0.96
EBZ	120%	24.0	99.75	0.77	0.77
MF	80%	1.6	99.38	0.027	1.66
MF	100%	2.0	99.67	0.035	1.76
MF	120%	2.4	100.14	0.041	1.69

Table. 16: Precision Results for EBZ and MF

Study	Drug	Nominal concentration (µg/mL)	Mean calculated (µg/mL)	SD	%RSD
Repeatability (n = 6)	EBZ	20	19.89	0.22	1.11
	MF	2	1.98	0.03	1.51
Intraday precision	EBZ	10	9.91	0.11	1.11
		20	19.95	0.17	0.85
		30	30.12	0.38	1.25
	MF	1	0.98	0.02	1.72
		2	1.97	0.03	1.52

		3	3.04	0.03	1.15
Intermediate precision	EBZ	10	9.85	0.14	1.45
		20	19.88	0.22	1.10
		30	29.95	0.35	1.18
	MF	1	1.02	0.02	1.85
		2	1.99	0.03	1.42
		3	2.97	0.04	1.48

Table.17: Sensitivity Parameters

Drug	Calibration slope	SD of intercept	LOD (µg/mL)	LOQ (µg/mL)
EBZ	0.0215	0.0053	0.82	2.48
MF	0.0342	0.0026	0.25	0.75

Accuracy was close to 100% and all reported precision values were below 2% RSD. The MF LOQ of 0.75 µg/mL allowed quantification at the lower formulation level, although early receptor samples below this value must be reported as below LOQ rather than as precise concentrations.

5.7 Robustness and operational suitability

Table.18: Robustness, Solution Stability, Filter Compatibility, and Extraction Recovery

Assessment	Condition	Eberconazole nitrate (EBZ)	Mometasone furoate (MF)
Robustness	Control (261/248 nm)	20.00 µg/mL; 0.9% RSD	2.00 µg/mL; 1.2% RSD
	260/247 nm	19.82 µg/mL; 1.2% RSD	1.96 µg/mL; 1.5% RSD
	262/249 nm	20.15 µg/mL; 1.1% RSD	2.03 µg/mL; 1.4% RSD
Solution stability	Ambient (4 h)	99.6% recovery	99.0% recovery
	Ambient (8 h)	99.2% recovery	98.5% recovery
	Ambient (24 h)	98.2% recovery	97.5% recovery
	Refrigerated (24 h, 4°C)	99.5% recovery	99.1% recovery
Filter compatibility	0.45 µm PVDF membrane	99.8 ± 0.5%	99.2 ± 0.8%
Extraction recovery	Methanol sonication (gel matrix)	98.4 ± 1.2%	97.9 ± 1.5%

5.8 Orthogonal HPLC comparison

Selected formulation extracts were also analysed with an Agilent 1260 Infinity II PDA system using a Waters XBridge C18 column (250 × 4.6 mm, 5 µm), acetonitrile-water (70:30 v/v), a flow rate of 1.0 mL/min, a column temperature of 25°C, a 20 µL injection, and detection at 250 nm. Approximate retention times were 4.2 minutes for EBZ and 6.8 minutes for MF.

Table.19: Agreement Between UV and HPLC Assay Results

Formulation	UV EBZ (%)	HPLC EBZ (%)	Difference (%)	UV MF (%)	HPLC MF (%)	Difference (%)
F1	100.0	99.1	0.90	100.0	98.2	1.83
F2	100.2	99.4	0.80	100.5	98.8	1.72
F3	100.4	100.1	0.30	101.0	99.5	1.50
F4	99.9	99.9	0.00	99.5	99.1	0.40

The percentage differences were below 2%. This close agreement provided orthogonal support for the accuracy of the simultaneous-equation assay. Taken together, the validation results showed acceptable performance for the analytical characteristics examined in this study.

5.9 Solubility-Screening Results

Equilibrium solubility screening was performed separately for both drugs in the candidate oils, surfactants, and co-surfactants. The results showed a consistent ranking across the two active ingredients. Capryol 90 gave the highest solubility among the oils, Tween 80 gave the highest solubility among the surfactants, and Transcutol P gave the highest solubility among the co-surfactants.

Table.20: Solubility of the Drugs in Candidate Oils

Oil	Eberconazole nitrate (mg/mL)	Mometasone furoate (mg/mL)
Capryol 90	168.42 ± 2.31	154.78 ± 2.16
Isopropyl myristate	141.65 ± 1.94	138.56 ± 1.89
Oleic acid	126.83 ± 2.12	121.43 ± 1.95
Labrafac Lipophile WL 1349	113.28 ± 1.87	109.37 ± 1.74
Capmul MCM	97.51 ± 1.56	93.81 ± 1.62
Castor oil	68.47 ± 1.43	66.52 ± 1.31

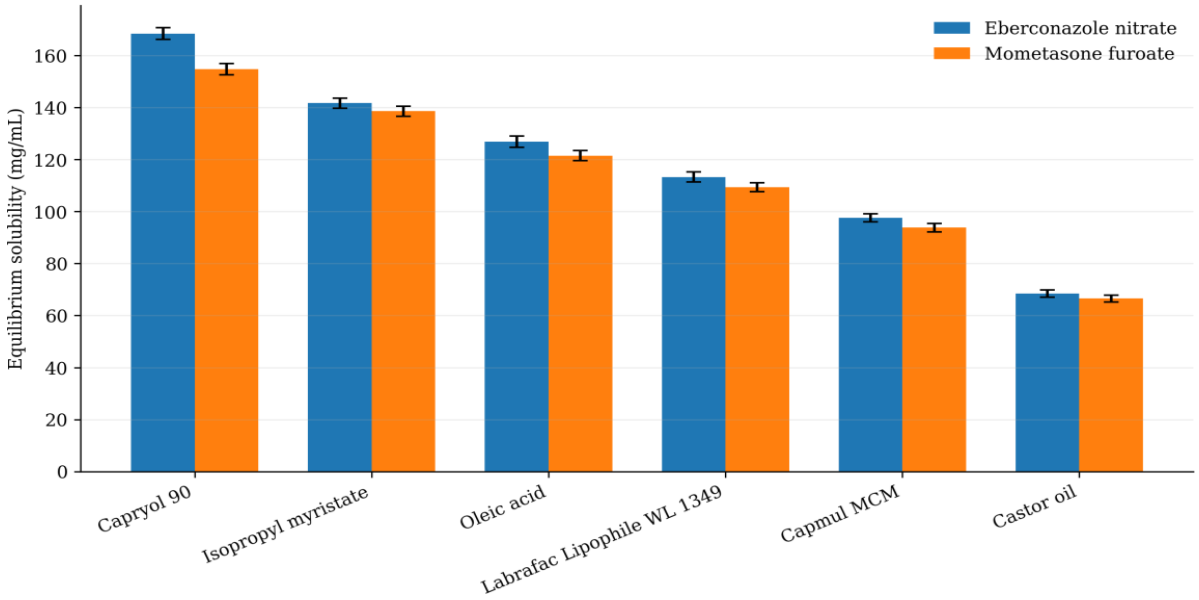

Figure.5: Comparative solubility of eberconazole nitrate and mometasone furoate in candidate oils (mean ± SD, n = 3).

Table.21: Solubility of the Drugs in Candidate Surfactants

Surfactant	Eberconazole nitrate (mg/mL)	Mometasone furoate (mg/mL)
Tween 80	215.36 ± 2.65	203.74 ± 2.47
Cremophor RH40	198.74 ± 2.43	191.68 ± 2.29
Kolliphor EL	176.58 ± 2.08	172.85 ± 2.13
Tween 20	162.91 ± 1.96	159.47 ± 1.84
Span 80	118.46 ± 1.72	114.83 ± 1.69

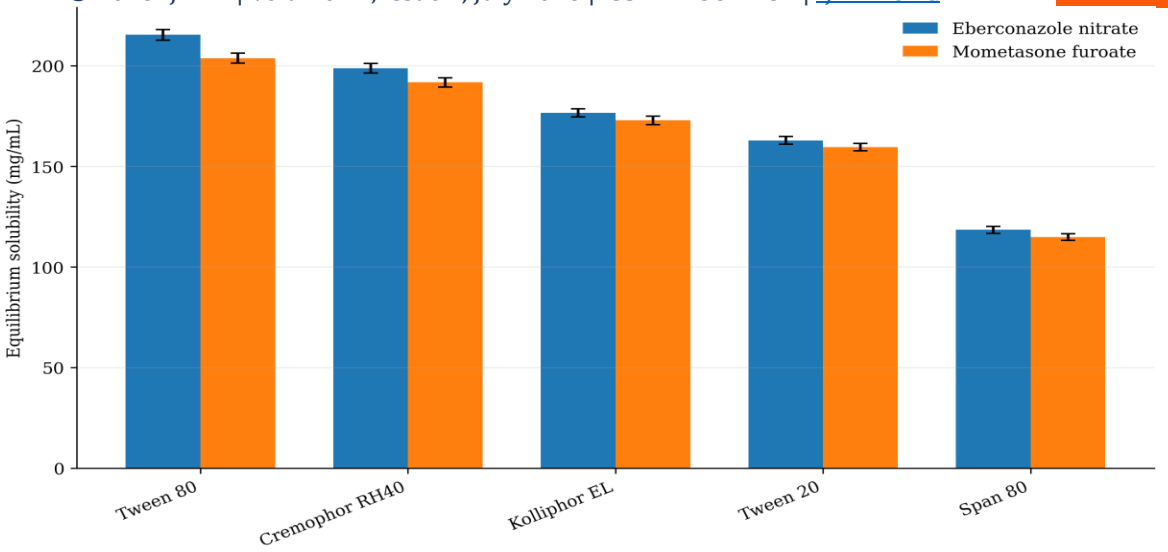

Figure.6: Comparative solubility of eberconazole nitrate and mometasone furoate in candidate surfactants (mean ± SD, n = 3).

Table.22: Solubility of the Drugs in Candidate Co-surfactants

Co-surfactant	Eberconazole nitrate (mg/mL)	Mometasone furoate (mg/mL)
Transcutol P	256.84 ± 2.58	241.35 ± 2.41
PEG 400	221.63 ± 2.34	216.72 ± 2.18
Propylene glycol	204.91 ± 2.11	197.54 ± 1.96
Ethanol	186.42 ± 1.97	181.26 ± 1.88
PEG 200	173.56 ± 1.82	169.81 ± 1.73

Capryol 90 dissolved 168.42 ± 2.31 mg/mL of eberconazole nitrate and 154.78 ± 2.16 mg/mL of mometasone furoate. These values were higher than those recorded for the other tested oils. Tween 80 dissolved 215.36 ± 2.65 mg/mL and 203.74 ± 2.47 mg/mL of the respective drugs. Transcutol P showed the greatest overall solubilizing capacity, with values of 256.84 ± 2.58 mg/mL for eberconazole nitrate and 241.35 ± 2.41 mg/mL for mometasone furoate.

5.11 ATR-FTIR Compatibility Results

ATR-FTIR spectra of the pure drugs and the best-performing microemulgel were compared to assess whether the main functional-group bands were retained after formulation. The principal peaks preserved in the experimental record are summarized in Table 23.

Table.23: Characteristic ATR-FTIR Bands of the Pure Drugs and F3 Microemulgel

Sample	Band (cm^{-1})	Assignment
Eberconazole nitrate	3062	Aromatic C–H stretching
	2928	Aliphatic C–H stretching
	1597	Imidazole C=N/aromatic C=C stretching
	1248	Ether C–O–C stretching
	1118	C–N stretching
	747	C–Cl stretching
Mometasone furoate	3441	O–H stretching
	2934	Aliphatic C–H stretching
	1732	Ester carbonyl stretching
	1664	Conjugated ketone stretching
	1605	C=C stretching

	1236	C–O stretching
	1110	C–F stretching
	753	C–Cl stretching
F3 Microemulgel	3434	Broadened O–H stretching
	2926	Aliphatic C–H stretching
	1728	Ester carbonyl stretching
	1661	Ketone carbonyl stretching
	1596	Imidazole C=N stretching
	1242	Ether/C–O stretching
	1114	C–N/C–F stretching
	748	C–Cl stretching

Figure.8: ATR-FTIR overlay spectrum of eberconazole nitrate, mometasone furoate, and F3 microemulgel.

5.12 Differential Scanning Calorimetry Results

Table.24: DSC Thermal Events of the Pure Drugs and F3 Microemulgel

Sample/event	Onset (°C)	Peak (°C)	Endset (°C)	ΔH (J/g)	Interpretation
Eberconazole nitrate	160.8	166.4	171.2	91.8	Sharp crystalline melting event
Mometasone furoate	216.9	222.2	227.8	79.6	Sharp crystalline melting event
F3 – eberconazole-associated event	159.7	164.8	169.6	36.9	Broadened event with reduced enthalpy
F3 – mometasone-associated event	218.4	220.3	224.8	29.7	Reduced peak intensity

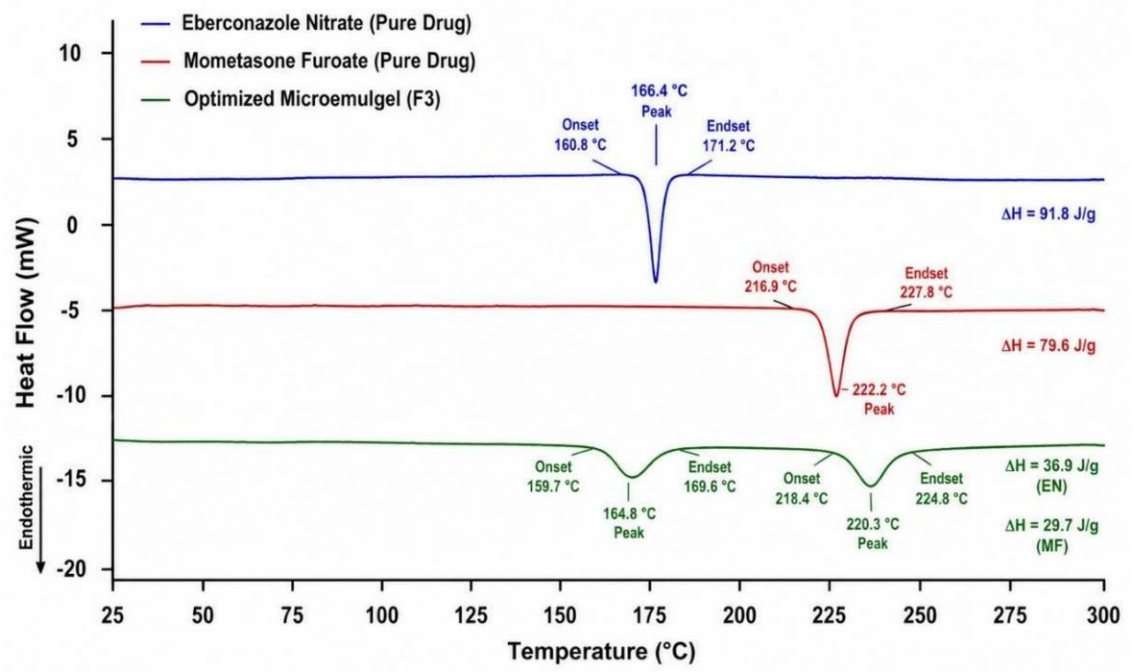

Figure.9: DSC thermograms of the pure drugs and F3 microemulgel

The pure drugs showed distinct endothermic events close to their measured melting points. In F3, the corresponding transitions were still identifiable but were broader and had lower enthalpy values. The reduced intensity is consistent with dilution of the drugs in the formulation and may also indicate partial loss of crystalline order or molecular dispersion. Because the drug concentration in the final microemulgel was much lower than in the pure-drug samples, reduced peak area should not be interpreted as proof of

complete amorphization.

5.13 X-Ray Diffraction Results

Table.25: Representative XRD Peaks of the Pure Drugs and F3 Microemulgel

Sample	Representative 2θ peaks (°)	Observation
Eberconazole nitrate	13.2, 18.5, 22.7, 26.4	Sharp, intense peaks
Mometasone furoate	10.8, 16.9, 21.3, 24.8	Distinct crystalline peaks
F3 microemulgel	13.1, 18.3, 22.5	Principal peaks retained with lower intensity and broadening

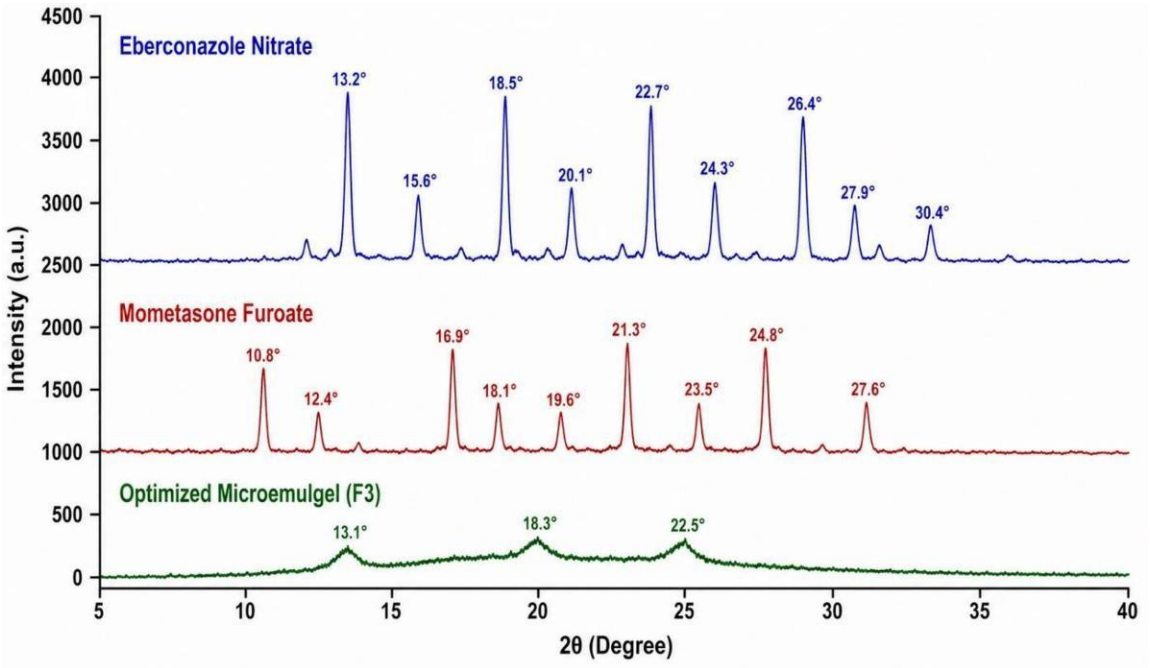

Figure.10: XRD patterns of eberconazole nitrate, mometasone furoate, and F3 microemulgel.

The pure drugs produced clear crystalline diffraction peaks. F3 retained several principal reflections, but their intensity was reduced and the background was more diffuse. The pattern supports partial reduction in crystalline order after incorporation into the microemulsion and Carbopol matrix. The absence of a new strong diffraction pattern suggests that no new dominant crystalline phase formed under the tested conditions. As with DSC, dilution and the large excipient fraction also contribute to the lower apparent peak intensity.

5.14 Pseudo-Ternary Phase-Diagram Results

Pseudo-ternary phase diagrams were used to compare the phase behaviour of Capryol 90, Tween 80–Transcutol P mixtures, and water. The retained diagrams showed that the size of the clear isotropic region depended strongly on the surfactant-to-co-surfactant ratio.

Table. 26: Comparative Phase-Diagram Observations for Different S_mix Ratios

S_mix ratio	Relative clear region	Recorded observation	Decision
1:1	Small	Transparent, but with a limited clear region	Not selected
2:1	Moderate	Clear and stable	Considered
3:1	Largest	Clear, transparent, and highly stable region	Selected
4:1	Moderate	Transparent, with a reduced aqueous region	Considered
1:2	Small	Slight turbidity at higher water content	Not selected
1:3	Very small	Early phase separation recorded	Not selected

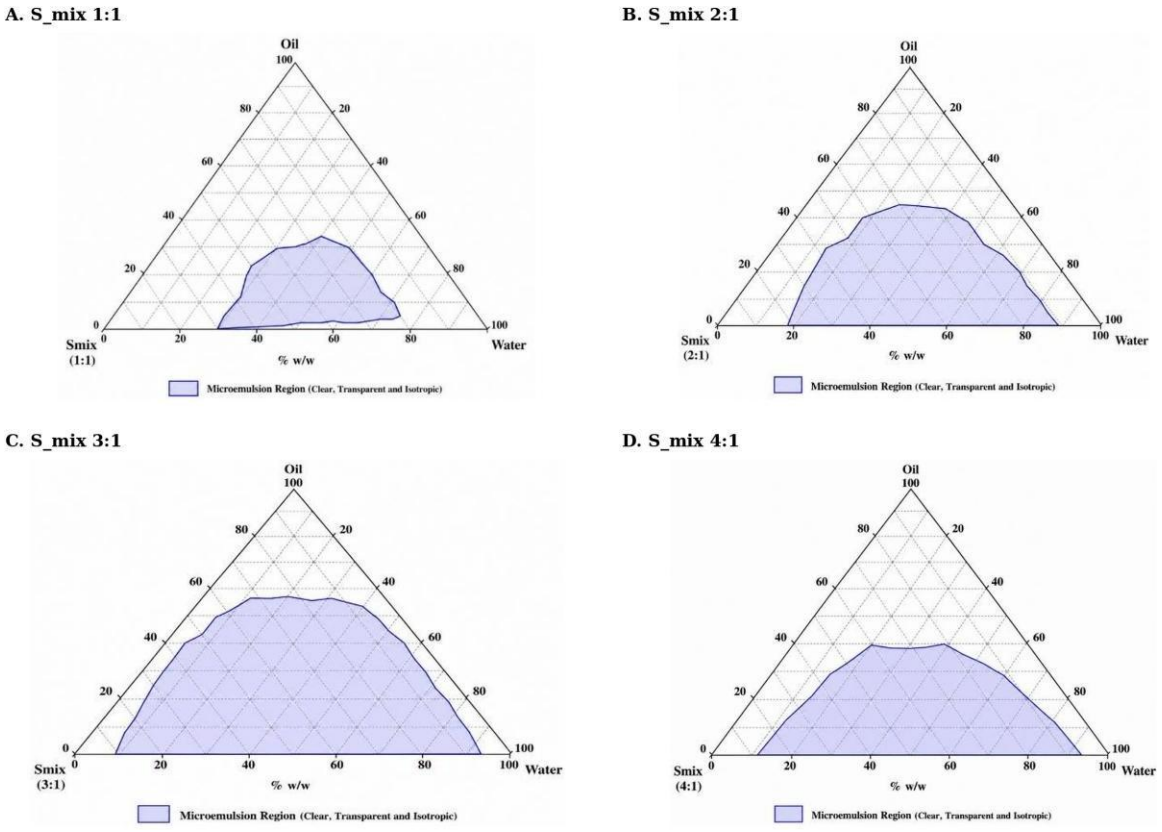

Figure. 11: Pseudo-ternary phase diagrams of the Capryol 90–S_mix–water system: (A) 1:1, (B) 2:1, (C) 3:1, and (D) 4:1 Tween 80:Transcutol P.

The 1:1 ratio gave only a limited clear region. Increasing the relative amount of Tween 80 to 2:1 expanded the region. The broadest preserved region occurred at 3:1, which provided the greatest flexibility for selecting oil, S_mix, and water proportions. A further increase to 4:1 reduced the region, suggesting that the additional surfactant did not provide a further phase-behaviour advantage under the tested conditions. The result supported the selection of the 3:1 S_mix ratio for F1–F4.

5.15 Preparation and Evaluation of F1–F4 Liquid Microemulsions

Table.27: Composition of the Drug-Loaded Liquid Microemulsions

Ingredient (% w/w)	F1	F2	F3	F4
Eberconazole nitrate	1.0	1.0	1.0	1.0
Mometasone furoate	0.1	0.1	0.1	0.1
Capryol 90	8	10	12	14
Tween 80	28	30	32	34
Transcutol P	9	10	11	12
Purified water	q.s. to 100	q.s. to 100	q.s. to 100	q.s. to 100

Table.28: Physicochemical Evaluation of the Liquid Microemulsions

Parameter	F1	F2	F3	F4
Appearance	Clear	Clear	Clear	Slightly opalescent
Transparency	Transparent	Transparent	Transparent	Slightly turbid
Phase separation	Absent	Absent	Absent	Absent
Transmittance (%)	96.18 ± 0.41	97.54 ± 0.32	99.12 ± 0.26	95.67 ± 0.48
pH	5.84 ± 0.04	5.93 ± 0.03	6.08 ± 0.02	6.14 ± 0.03
Conductivity (µS/cm)	218.4 ± 3.2	235.7 ± 2.8	247.6 ± 2.4	241.8 ± 2.6
Refractive index	1.426 ± 0.002	1.431 ± 0.002	1.436 ± 0.001	1.438 ± 0.002
Viscosity (cP)	74.3 ± 1.6	81.5 ± 1.9	88.6 ± 1.7	96.4 ± 2.2
Apparent combined content (%)	96.82 ± 0.71	98.14 ± 0.58	99.41 ± 0.43	97.36 ± 0.64

Table.29: Physical-Stress Test Results of the Liquid Microemulsions

Formulation	Centrifugation	Heating–cooling cycles	Freeze–thaw cycles	Overall observation
F1	Passed	Passed	Passed	Stable under applied tests
F2	Passed	Passed	Passed	Stable under applied tests
F3	Passed	Passed	Passed	Stable under applied tests
F4	Passed	Passed	Passed	Stable under applied tests

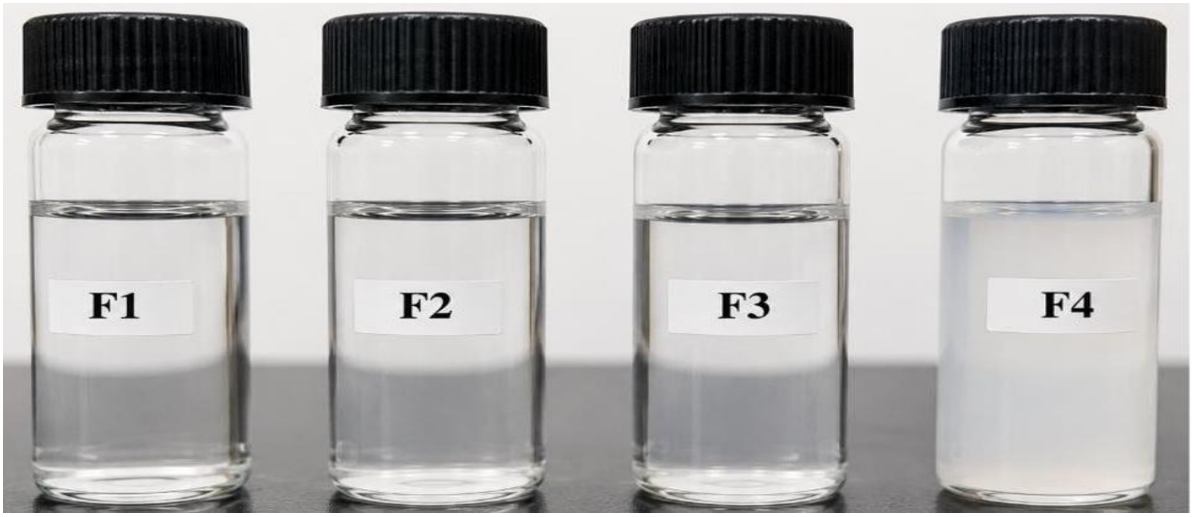

Figure. 12: Prepared liquid formulations F1–F4. F4 showed visible opalescence relative to F1–F3.

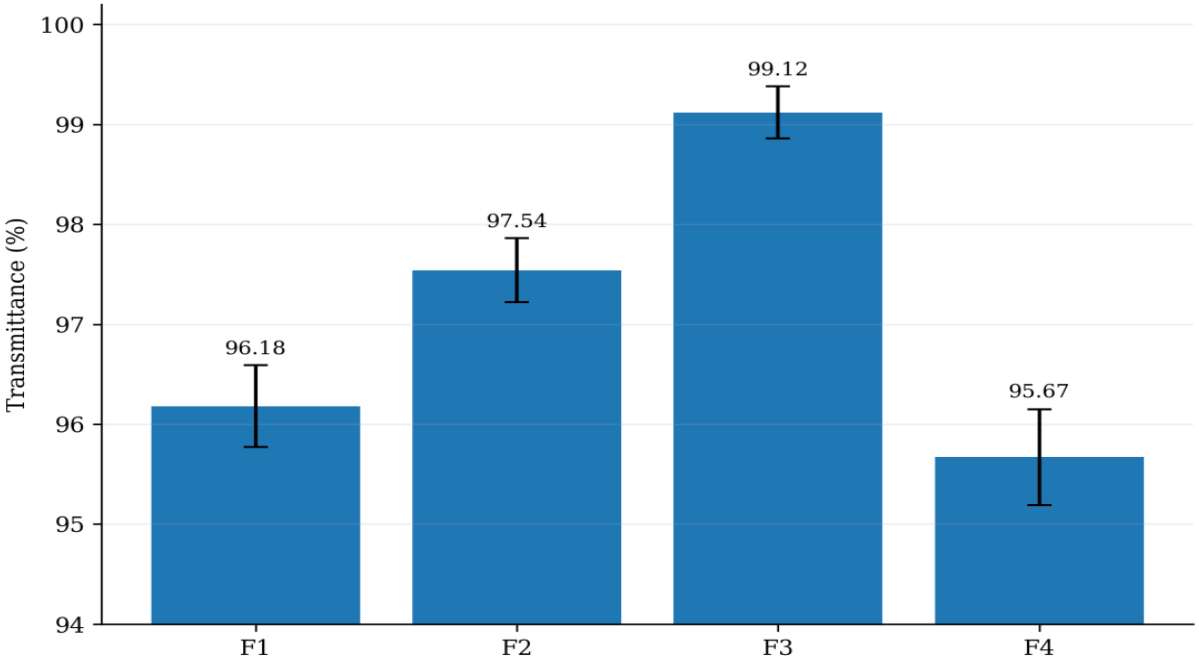

Figure.13: Percentage transmittance of F1–F4 (mean ± SD, n = 3).

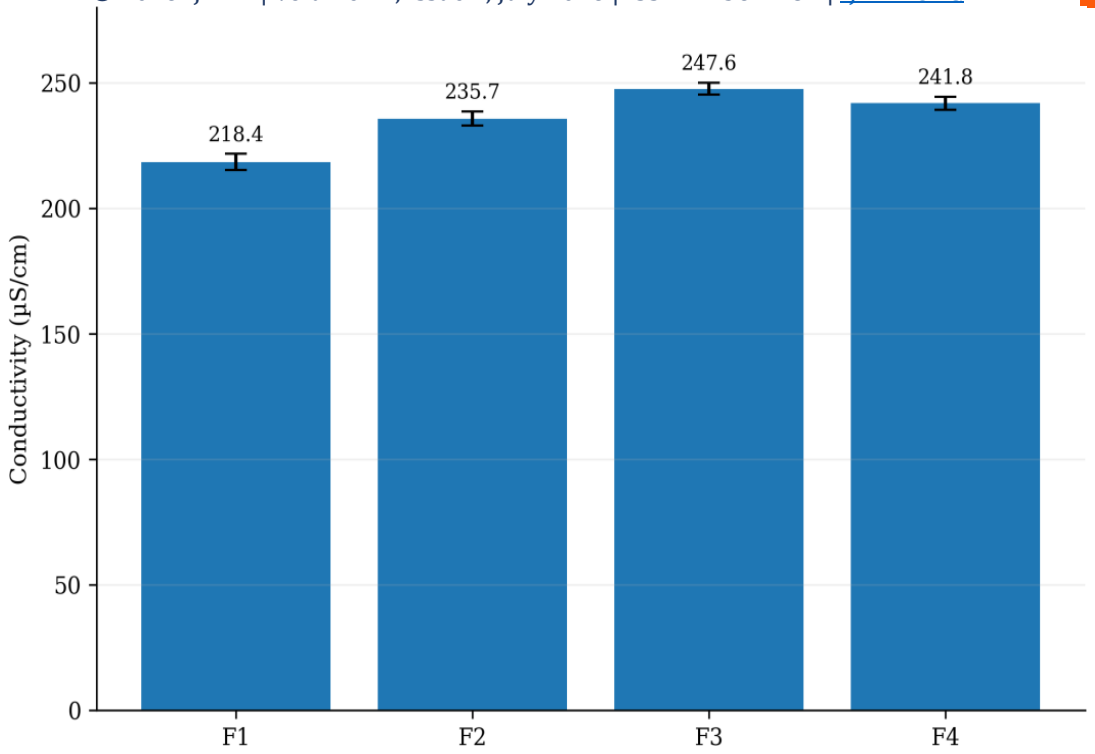

Figure.14: Conductivity of F1–F4 (mean ± SD, n = 3).

F1–F4 showed good physical stability. F3 exhibited optimal clarity (99.12% transmittance), content recovery (99.41%), pH (6.08), moderate viscosity, and superior overall formulation quality.

5.16 Advanced Characterization of F3

Table.30: Advanced Characterization Results of F3

Parameter	**Recorded Result**
Mean hydrodynamic diameter by DLS (nm)	148.6 ± 3.2
Polydispersity index	0.128 ± 0.009
Zeta potential (mV)	−32.8 ± 1.4
TEM morphology	Spherical droplets with smooth surfaces
Average diameter by TEM (nm)	135.4 ± 4.1

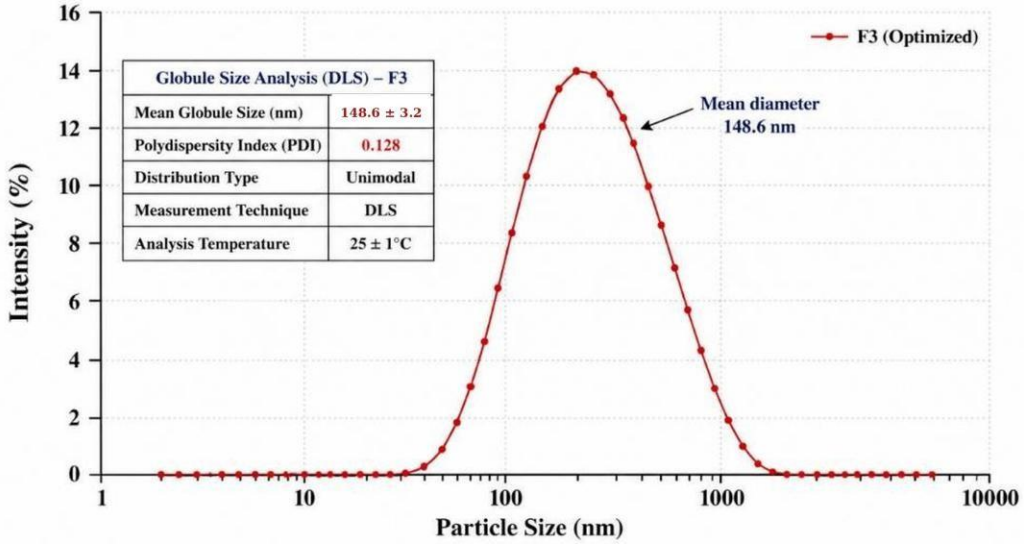

Figure. 15: DLS particle-size distribution of F3.

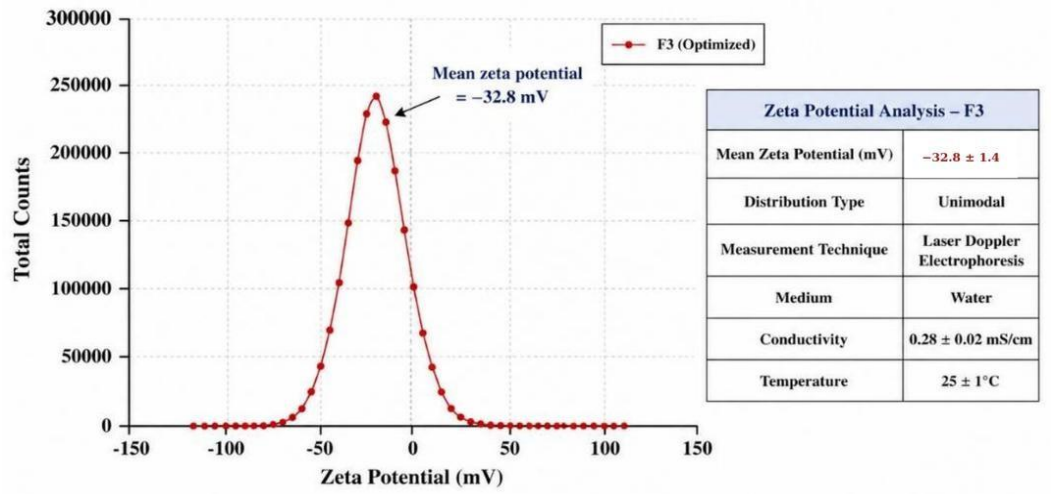

Figure.16: Zeta-potential distribution of F3.

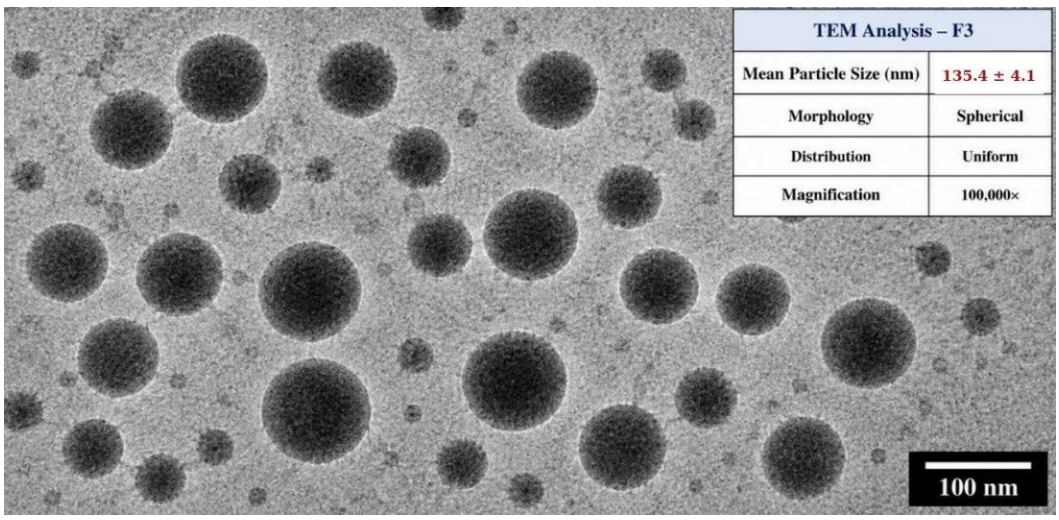

Figure.17: TEM micrograph of F3 showing approximately spherical droplets.

3 exhibited nanoscale droplets with DLS size of 148.6 ± 3.2 nm, low PDI (0.128 ± 0.009), and zeta potential of −32.8 ± 1.4 mV, indicating a uniform and stable colloidal system.

TEM confirmed smooth spherical droplets with a diameter of 135.4 ± 4.1 nm, supporting the successful development of a homogeneous nanoscale microemulgel formulation.

5.17 Evaluation of F1–F4 Microemulgels

Each complete drug-loaded microemulsion concentrate was converted directly into its correspondingly coded Carbopol 940 microemulgel. The resulting microemulgels were assessed for appearance, pH, viscosity, spreadability, extrudability, and the individual assay of EBZ and MF.

Table .18: Physicochemical Evaluation of the Microemulgels

Parameter	F1	F2	F3	F4
Appearance	Smooth	Smooth	Smooth	Smooth
Colour	Off-white	Off-white	Off-white	Off-white
Homogeneity	Good	Good	Excellent	Good
Grittiness	Absent	Absent	Absent	Absent
pH	5.86 ± 0.04	5.94 ± 0.03	6.02 ± 0.02	6.08 ± 0.03
Viscosity (cP)	28,420 ± 214	30,185 ± 238	32,746 ± 195	34,218 ± 231
Spreadability (g·cm/s)	16.84 ± 0.36	18.12 ± 0.31	19.64 ± 0.28	17.53 ± 0.33
Extrudability (g/cm²)	508 ± 11	536 ± 10	571 ± 9	548 ± 10
Apparent Combined Drug Content (%)	97.21 ± 0.64	98.08 ± 0.51	99.32 ± 0.38	98.54 ± 0.47

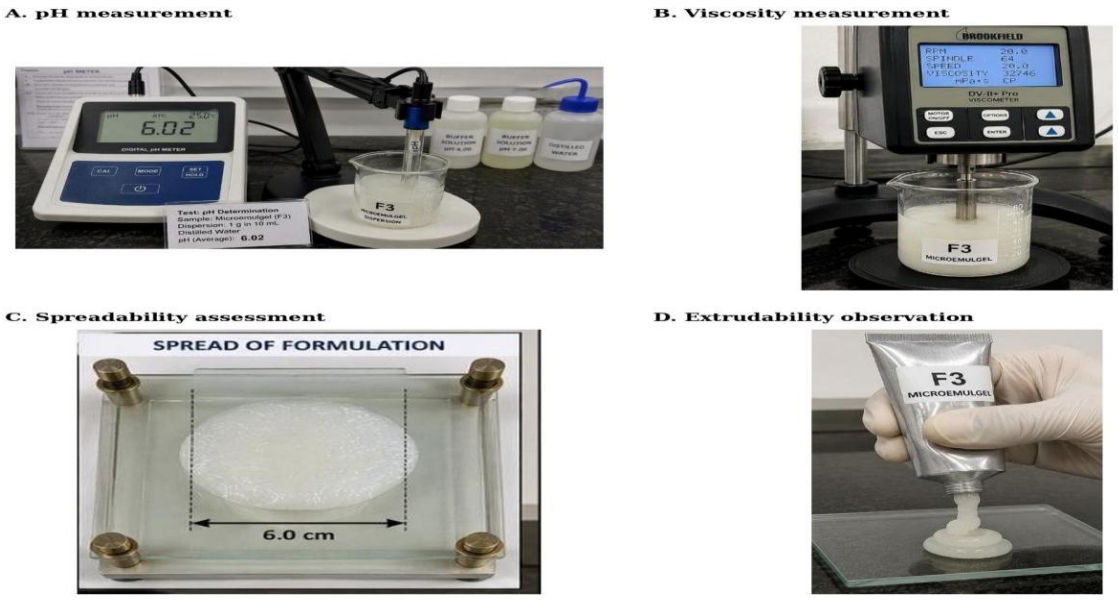

Figure 6.19. Individual EBZ and MF assay values of F1-F4 microemulgels (mean ± SD, n = 3).

All formulations were smooth, off-white, homogeneous, and free from grittiness. The pH ranged from 5.86 ± 0.04 to 6.08 ± 0.03, with F3 (6.02 ± 0.02) showing excellent homogeneity and remaining within the acceptable range for topical application. Viscosity increased from F1 (28,420 ± 214 cP) to F4 (34,218 ± 231 cP); however, F3 exhibited the highest spreadability (19.64 ± 0.28 g·cm/s) and extrudability (571 ± 9 g/cm²), indicating an optimal balance between consistency and ease of application. Drug content was satisfactory in all formulations, with F3 showing the highest apparent combined drug content (99.32 ± 0.38%), confirming uniform drug distribution.

5.18 In-Vitro Apparent Combined Release Through Dialysis Membrane

The release study compared the four microemulgels over 12 hours using a Franz diffusion-cell assembly fitted with a dialysis membrane. A validated dual-wavelength UV method was available for drug-specific analysis; however, the complete A_1 and A_2 records required to reconstruct separate F1-F4 cumulative profiles were not preserved at every sampling point. The historical comparative dataset was therefore retained as an apparent combined response for batch comparison.

Table. 19: Apparent Cumulative Combined Release from F1–F4

e (h)	F1 (%)	F2 (%)	F3 (%)	F4 (%)
0.5	12.84 ± 0.62	15.43 ± 0.54	17.28 ± 0.48	13.95 ± 0.57
1	21.36 ± 0.75	25.82 ± 0.68	29.41 ± 0.63	23.74 ± 0.70
2	34.58 ± 0.88	40.65 ± 0.81	46.12 ± 0.74	38.37 ± 0.84
3	45.71 ± 0.91	52.84 ± 0.86	59.83 ± 0.79	50.48 ± 0.88
4	56.83 ± 0.95	64.42 ± 0.92	71.26 ± 0.83	61.74 ± 0.91
6	68.27 ± 1.04	75.68 ± 0.98	82.74 ± 0.90	73.65 ± 0.96
8	77.84 ± 1.08	84.32 ± 1.02	90.53 ± 0.96	82.48 ± 1.01
10	84.16 ± 1.11	89.37 ± 1.05	95.74 ± 1.01	88.21 ± 1.04
12	89.52 ± 1.15	93.28 ± 1.08	98.36 ± 0.94	91.84 ± 1.09

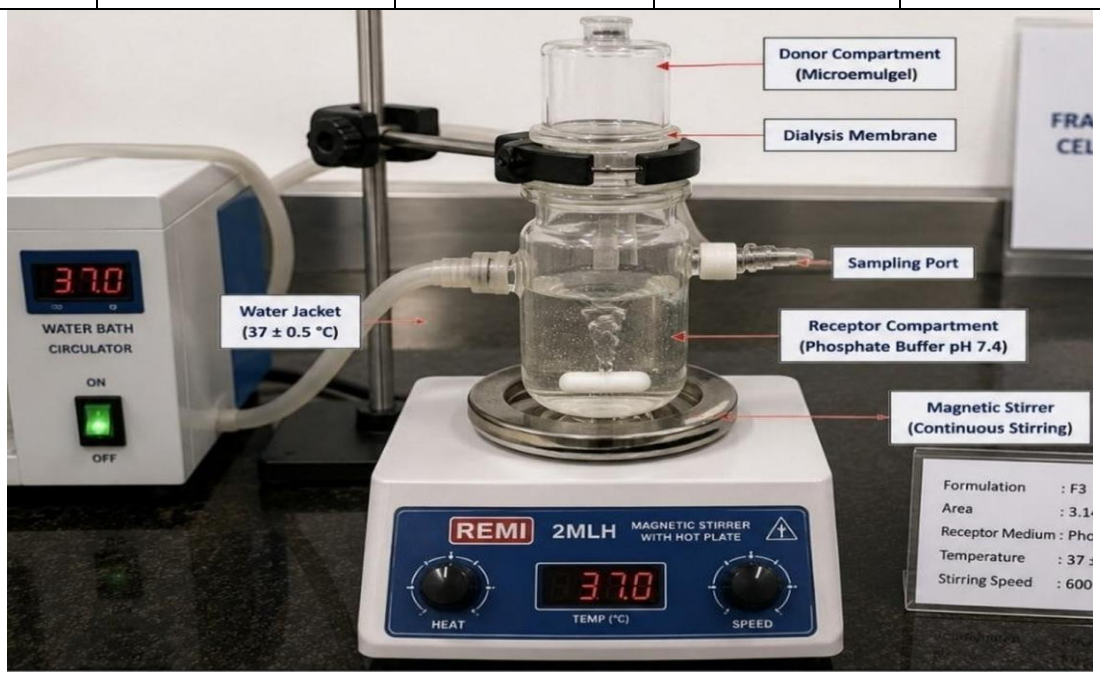

Figure. 18: Franz diffusion-cell assembly used for the dialysis-membrane release study.

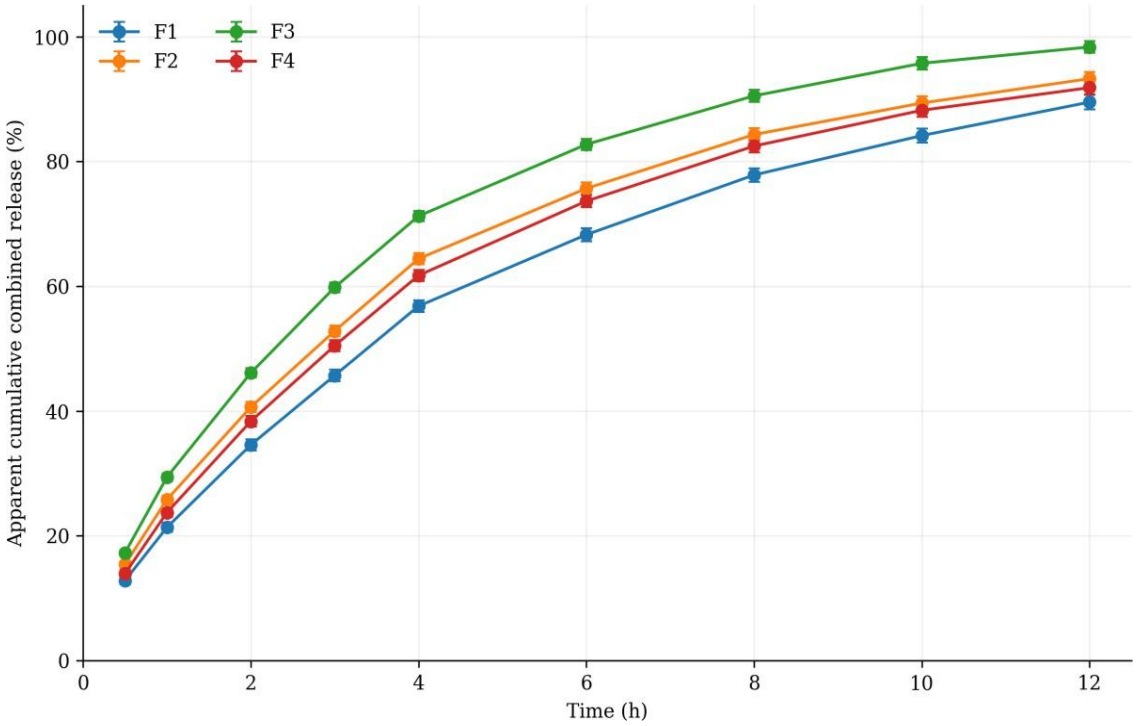

Figure. 19: Combined release profiles of F1–F4 over 12 hours (mean ± SD, n = 3).

All formulations showed sustained drug release over 12 hours. F3 exhibited the highest cumulative release, increasing from 17.28 ± 0.48% at 0.5 hour to 98.36 ± 0.94% at 12 hours. At the end of the study, the release order was F3 > F2 > F4 > F1, with low standard deviations indicating good reproducibility. The superior release from F3 may be attributed to its optimal balance of drug solubilization, droplet distribution, and gel consistency. Although F4 had higher oil and S_{mix} content and greater viscosity, its release was lower than F3, suggesting that increasing liquid components alone did not enhance drug release. Since the study was performed using a dialysis membrane, the results represent in-vitro drug release rather than skin permeation or dermal absorption.

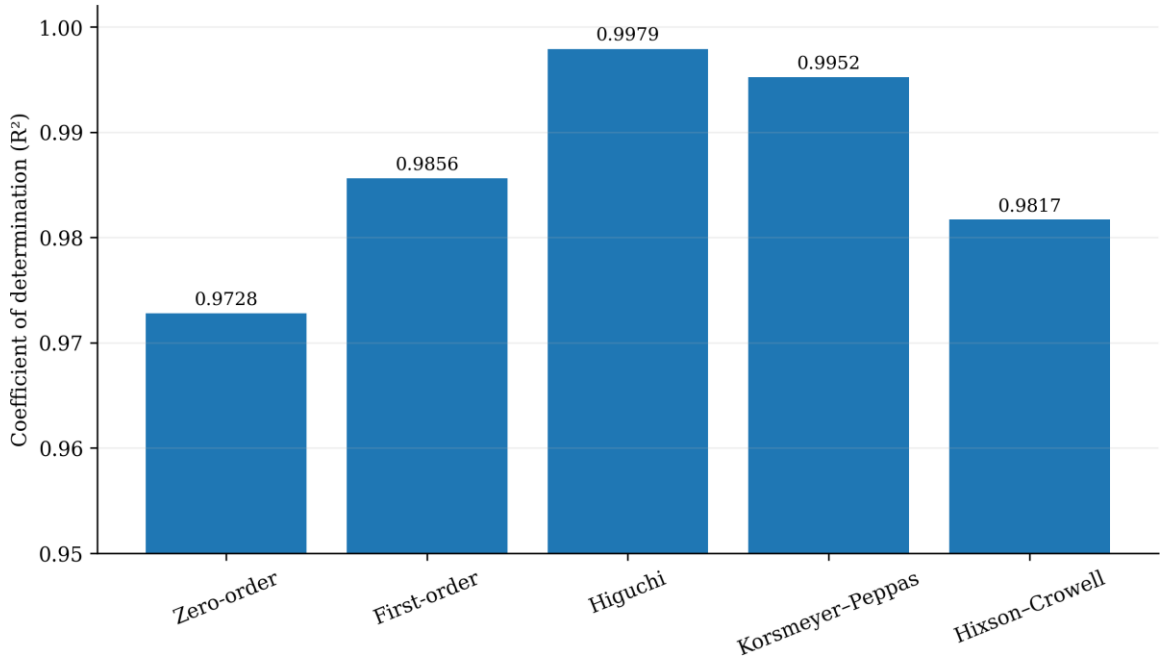

Figure. 2 0 : Comparison of the coefficients of determination obtained for the fitted release models.

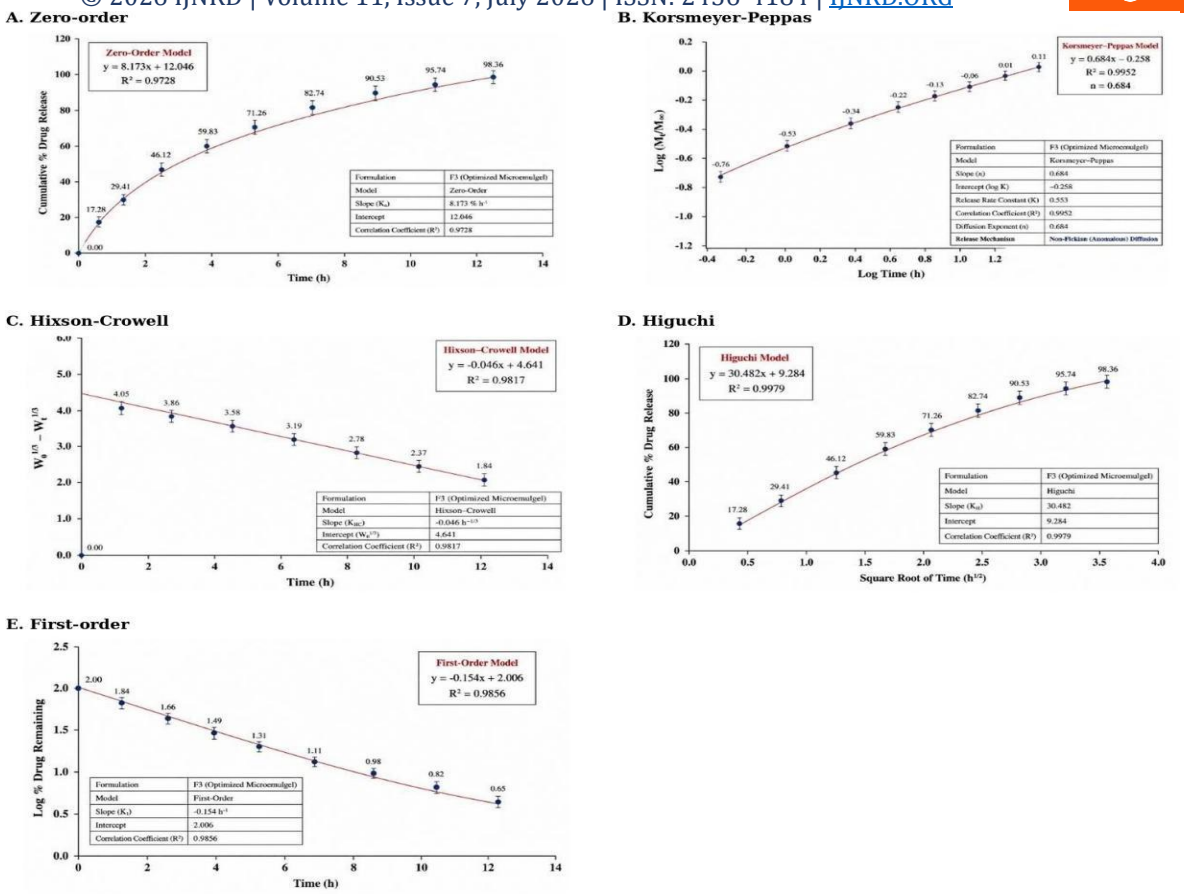

Figure.21: Kinetic plots fitted to the preserved comparative release response from F3.

5.19 Minimum Inhibitory Concentration (MIC) Against *Trichophyton rubrum*

Table 20:MIC Results Against *T. rubrum*

Test Sample	Recorded MIC (µg/mL)
Pure eberconazole nitrate	2.0
F3 microemulgel	1.0
Marketed formulation	2.0

The F3 microemulgel exhibited the lowest MIC (1.0 µg/mL). In contrast, pure eberconazole nitrate and the marketed formulation showed MIC values of 2.0 µg/mL, indicating enhanced antifungal activity of F3 under the experimental conditions. The antifungal effect is primarily attributed to eberconazole nitrate, while mometasone furoate contributed only its anti-inflammatory role. The findings support improved drug availability in the formulation but do not establish clinical superiority or skin efficacy.

5.20 Overall Interpretation and Selection of F3

Table.21: Main Findings Supporting the Selection of F3

Selection Attribute	**F3 Result**
Liquid microemulsion clarity	99.12 ± 0.26% transmittance
Drug content (liquid)	99.41 ± 0.43%
Physical stability	Passed centrifugation, heating–cooling, and freeze–thaw tests
Droplet size (DLS)	148.6 ± 3.2 nm (PDI 0.128 ± 0.009)
Zeta potential	−32.8 ± 1.4 mV
TEM	Spherical droplets (135.4 ± 4.1 nm)
pH	6.02 ± 0.02
Spreadability	19.64 ± 0.28 g·cm/s
Extrudability	571 ± 9 g/cm²
Drug content (microemulgel)	99.32 ± 0.38%

12-hour drug release	98.36 ± 0.94%
Release kinetics	Higuchi (R^2 = 0.9979); Korsmeyer–Peppas (n = 0.684)
Antifungal activity	MIC 1.0 µg/mL against *T. rubrum*

F3 demonstrated the best overall balance of physicochemical properties, stability, drug release, and antifungal activity. Although F4 showed higher viscosity, its transparency and drug release were lower than F3, while F1 and F2 exhibited comparatively lower content, spreadability, and release. Based on the combined evaluation, F3 was selected as the optimized formulation.

Preformulation studies confirmed drug compatibility and identified Capryol 90, Tween 80, and Transcutol P (3:1) as the optimized microemulsion system. ATR-FTIR, DSC, and XRD indicated successful incorporation of both drugs without significant incompatibility. Among all formulations, F3 showed superior clarity, stability, droplet characteristics, pH, spreadability, extrudability, drug content, 98.36 ± 0.94% drug release at 12 hours, and the lowest MIC (1.0 µg/mL) against *T. rubrum*. Drug release followed the Higuchi and Korsmeyer–Peppas models, supporting diffusion-controlled release. Overall, these findings identify F3 as the optimized dual-drug microemulgel, while further skin permeation, long-term stability, and clinical studies are required to confirm its therapeutic performance.

5. CONCLUSION

A dual-drug microemulgel containing eberconazole nitrate and mometasone furoate was successfully developed and optimized. Among four formulations, F3 showed superior physicochemical properties, nanosized droplets, uniform drug content, sustained drug release (98.36 ± 0.94% at 12 h), and the lowest MIC (1.0 µg/mL) against *Trichophyton rubrum*. These findings suggest that F3 is a promising topical formulation for inflammatory fungal infections. Further skin permeation, stability, in-vivo, and clinical studies are needed to confirm its therapeutic potential.

6. FUTURE PERSPECTIVES

The study was limited to laboratory-scale formulation development, in-vitro dialysis membrane release, and antifungal evaluation against a single fungal species. Long-term stability, skin permeation, anti-inflammatory activity, safety, and clinical efficacy were not investigated. Future studies should employ Quality-by-Design optimization, biological skin permeation models, comprehensive stability testing, expanded microbiological evaluation, and preclinical and clinical investigations to validate the formulation for therapeutic use.

7. REFERENCES

[1] S. P. Payyal, N. C. Rompicherla, S. D. Sathyanarayana, R. G. Shriram, and A. N. Vadakkepushpakath, “Microemulsion based gel of sulconazole nitrate for topical application,” *Turkish J. Pharm. Sci.*, vol. 17, no. 3, pp. 259–264, Jun. 2020, doi: 10.4274/tjps.galenos.2019.75537.

[2] S. Dogra and S. Uprety, “The menace of chronic and recurrent dermatophytosis in India: Is the problem deeper than we perceive?,” *Indian Dermatol. Online J.*, vol. 7, p. 73, 2016, doi: 10.4103/2229-5178.178100.

[3] K. Sahni, S. Singh, and S. Dogra, “Newer topical treatments in skin and nail dermatophyte infections,” *Indian Dermatol. Online J.*, vol. 9, p. 149, 2018, doi: 10.4103/idoj.IDOJ_281_17.

[4] S. B. Verma *et al.*, “The unprecedented epidemic-like scenario of dermatophytosis in India: I. Epidemiology, risk factors and clinical features,” Mar. 2021, *Scientific Scholar*. doi: 10.25259/IJDVL_301_20.

[5] D. Mijaljica, F. Spada, and I. P. Harrison, “Emerging Trends in the Use of Topical Antifungal-Corticosteroid Combinations,” Aug. 2022, *MDPI*. doi: 10.3390/jof8080812.

[6] P. Shah Dhiren and K. Patel Heta, “Design, development and characterization of microemulsion based hydrogel of mometasone furoate for topical delivery system,” *Int. J. Pharm. Res.*, vol. 12, no. 2, pp. 1502–1515, 2020.

[7] "Seborrheic Dermatitis and Dandruff: A Comprehensive Review," *J. Clin. Investig. Dermatology*, vol. 3, 2015, doi: 10.13188/2373-1044.1000019.
[8] V. Jadhav, P. M. Mane, and S. R. Patil, "Steroid-Modified Dermatophytosis: A Clinical and Diagnostic Challenge," *Cureus*, May 2026, doi: 10.7759/cureus.108993.
[9] A. K. Bubna, "Topical Azole Antifungal drugs," in *Therapeutics in Dermatology - Essentials for Clinical Practice*, Springer Nature Singapore, 2025, pp. 87–104. doi: 10.1007/978-981-95-3803-4_8.
[10] B. Biswas and A. Thakur, "Fungal fighters: A comprehensive guide to antifungal therapies of the past, present, and future," in *Recent Advances in Human Fungal Diseases: Progress and Prospects*, Springer Nature, 2024, pp. 43–64. doi: 10.1007/978-981-97-4909-6_2.
[11] S. Bhargava *et al.*, "Rising burden of superficial fungal infections in India and the role of Clotrimazole for optimal management," 2023, *IP Innovative Publication Pvt. Ltd.* doi: 10.18231/j.ijced.2023.001.
[12] R. Gnaneshwar *et al.*, "The Efficacy and Safety of Eberconazole Nitrate 1% and Mometasone Furoate 0.1% w/w Cream in Subjects with Inflamed Cutaneous Mycoses," *Rev. Recent Clin. Trials*, vol. 10, pp. 161–170, Jul. 2015, doi: 10.2174/1574887110021507141412 34.
[13] P. Boonme, J. Kaewbanjong, T. Amnuaikit, T. Andreani, A. M. Silva, and E. B. Souto, "Microemulsion and Microemulsion-Based Gels for Topical Antifungal Therapy with Phytochemicals," *Curr. Pharm. Des.*, vol. 22, pp. 4257–4263, Jun. 2016, doi: 10.2174/1381612822666160603015436.
[14] J. Musakhanian, D. W. Osborne, and J. D. Rodier, "Skin Penetration and Permeation Properties of Transcutol® in Complex Formulations," Oct. 2024, *Springer Science and Business Media Deutschland GmbH*. doi: 10.1208/s12249-024-02886-8.
[15] N. Shah, K. Patel, and I. Singhvi, "Topical Delivery of Eberconazole Nitrate Loaded Microemulsion: Formulation, Design and Evaluation," *Int. J. Pharm. Sci. Drug Res.*, vol. 15, no. 4, pp. 478–487, 2023, doi: 10.25004/ijpsdr.2023.150412.
[16] A. Balmanno, J. R. Falconer, H. G. Ravuri, and P. C. Mills, "Strategies to Improve the Transdermal Delivery of Poorly Water-Soluble Non-Steroidal Anti-Inflammatory Drugs," May 2024, *Multidisciplinary Digital Publishing Institute (MDPI)*. doi: 10.3390/pharmaceutics16050675.
[17] N. Ahamad Ansair, J. Narayan Mishra, and D. Kumar Vishwakarma, "FORMULATION AND EVALUATION OF ANTIFUNGAL MICRO EMULSION-BASED GEL FOR TOPICAL DRUG DELIVERY USING MILLETIAPINNATA," *Int. J. Adv. Res.*, vol. 10, pp. 680–694, Sep. 2022, doi: 10.21474/ijar01/15409.
[18] S. Nurcahya, Y. Pranata, M. N. Pratamarta, N. Hidayati, and A. Setiawansyah, "Influence of Stearic Acid and Triethanolamine on the Physical Properties and Antibacterial Efficacy of Ocimum basilicum L. Anti-acne Cream against Staphylococcus epidermidis," *J. Food Pharm. Sci.*, pp. 439–459, Dec. 2025, doi: 10.22146/jfps.25043.
[19] T. R. Mudyahoto, O. A. Omoteso, S. M. Khamanga, and R. B. Walker, "Formulation development and optimization of artemether-lumefantrine self-nanoemulsifying drug delivery systems," *Pharmazie*, vol. 80, pp. 39–50, Aug. 2025, doi: 10.1691/ph.2025.5008.
[20] D. Mohapatra, S.-Y. Seo, and T. W. Corson, "Development and characterization of a topical ferrochelatase inhibitor nanoemulsion for choroidal neovascularization therapy," *Int. J. Pharm. X*, vol. 12, p. 100619, Dec. 2026, doi: 10.1016/j.ijpx.2026.100619.
[21] N. Sharma, S. Rao, and B. Vaghela, "Validated stability-indicating high-performance liquid chromatographic method for estimation of degradation behaviour of eberconazole nitrate and mometasone furoate in cream formulation," *Indian J. Pharm. Sci.*, vol. 75, pp. 76–82, Jan. 2023, doi: 10.4103/0250-474X.113530.
[22] A. A. Bunaciu, V. D. Hoang, and H. Y. Aboul-Enein, "Fourier transform infrared spectroscopy used in drug excipients compatibility studies," 2025, *Taylor and Francis Ltd.* doi: 10.1080/05704928.2024.2438747.

[23] N. Vinith Kumar, C. Arunkumar, and S. Srinivasa Senthil, "Experimental Study on Mechanical and Thermal Behavior of Foamed Concrete," in *Materials Today: Proceedings*, Elsevier Ltd, 2018, pp. 8753–8760. doi: 10.1016/j.matpr.2017.12.302.

[24] Z. X. Phuna, S. Vijayabalan, B. P. Panda, N. K. H. Shivashekaregowda, M. F. Shaikh, and P. Madhavan, "Improved cognition and memory via PLGA nanoparticle-mediated delivery of curcumin and piperine in an in vivo Alzheimer's disease model," *Drug Deliv. Transl. Res. 2025 1511*, vol. 15, no. 11, pp. 4314–4337, Aug. 2025, doi: 10.1007/S13346-025-01945-2.

[25] L. Miguel-Escuder *et al.*, "Use of Nicergoline as Adjunctive Treatment of Neurotrophic Keratitis in Routine Clinical Practice: A Case Series," *Ocul. Immunol. Inflamm.*, vol. 30, no. 7–8, pp. 1926–1930, Nov. 2022, doi: 10.1080/09273948.2021.1976214;SUBPAGE:STRING:ACCESS.

[26] A. M. Al-mahallawi, D. Ahmed, M. Hassan, and D. A. El-Setouhy, "Enhanced ocular delivery of clotrimazole via loading into mucoadhesive microemulsion system: In vitro characterization and in vivo assessment," *J. Drug Deliv. Sci. Technol.*, vol. 64, Aug. 2021, doi: 10.1016/j.jddst.2021.102561.

[27] G. Coneac *et al.*, "Development and Evaluation of New Microemulsion-Based Hydrogel Formulations for Topical Delivery of Fluconazole," *AAPS PharmSciTech*, vol. 16, no. 4, pp. 889–904, 2015, doi: 10.1208/s12249-014-0275-8.

[28] M. Daryab, M. Faizi, A. Mahboubi, and R. Aboofazeli, "Preparation and Characterization of Lidocaine-Loaded, Microemulsion-Based Topical Gels.," *Iran. J. Pharm. Res. IJPR*, vol. 21, p. e123787, Dec. 2022, doi: 10.5812/ijpr.123787.

[29] M. A. Shewaiter, T. M. Hammady, A. El-Gindy, S. H. Hammadi, and S. Gad, "Formulation and characterization of leflunomide/diclofenac sodium microemulsion base-gel for the transdermal treatment of inflammatory joint diseases," *J. Drug Deliv. Sci. Technol.*, vol. 61, Feb. 2021, doi: 10.1016/j.jddst.2020.102110.

[30] M. Shruti, D. Salphale, N. S. Bhajipale, P. Harish, and K. Kunjwani, "Formulation And Evaluation Of Emulgel For Topical Delivery Of Drug," 2025. [Online]. Available: www.ijrti.org

[31] B. A. Khan *et al.*, "Fabrication and Characterizations of Pharmaceutical Emulgel Co-Loaded with Naproxen-Eugenol for Improved Analgesic and Anti-Inflammatory Effects.," *Gels (Basel, Switzerland)*, vol. 8, Sep. 2022, doi: 10.3390/gels8100608.